

Manuscript Number: COGE-D-15-00787R1

Title: An Analytical Approach for the Prediction of Single Pile and Pile Group Behaviour in Clay

Article Type: Research Paper

Keywords: settlement; pile interaction; pile groups; nonlinear; analytical

Corresponding Author: Dr. Bryan Anthony McCabe, BA BAI PhD

Corresponding Author's Institution: College of Engineering and Informatics, National University of Ireland, Galway

First Author: Brian Blaise Sheil

Order of Authors: Brian Blaise Sheil; Bryan McCabe

Abstract: In this paper, the t-z method is employed to describe the nonlinear behaviour of a single pile and is used to obtain simplified predictions of pile group behaviour by considering the interaction between two-piles in conjunction with the Interaction Factor Method (IFM). The principal inconvenience of the t-z method arises from the determination of the resisting curve's shape; an improvement upon this aspect is the main aim of this study. Partial slip is considered using a new analytical approach which is an adaptation of a model based on bond degradation. Pile installation effects and interface strength reduction are uncoupled and considered explicitly in this study. Lateral profiles of mean effective stress after pile installation and subsequent consolidation which were representative of predictions determined in a previous study using a modified version of the cavity expansion method (CEM) are adopted; these predictions are subsequently used to relate installation effects to changes in soil strength and stiffness. In addition, the 'reinforcing' effects of a second, 'receiver', pile on the free-field soil settlement is considered using a nonlinear iterative approach where the relative pile-soil settlement along the pile shaft is related to the soil spring stiffness. Through comparisons with previously published field test data and numerical simulations, the results indicate that the proposed approach provides a sufficiently accurate representation of pile behaviour while conserving considerable computing requirements.

An Analytical Approach for the Prediction of Single Pile and Pile Group Behaviour in Clay

Brian B. Sheil¹ and Bryan A. McCabe^{2*}

¹ Postdoctoral researcher, Department of Engineering Science, University of Oxford, Parks Road, Oxford, OX1 3PJ, U.K. (formerly PhD Candidate, National University of Ireland, Galway).

²Lecturer, College of Engineering and Informatics, National University of Ireland, Galway, University Road, Newcastle, Galway, Ireland.

*Corresponding author. Email: bryan.mccabe@nuigalway.ie; Tel.: +353 (0)91 492021

Abstract

In this paper, the ‘t-z method’ is employed to describe the nonlinear behaviour of a single pile and is used to obtain simplified predictions of pile group behaviour by considering the interaction between two-piles in conjunction with the Interaction Factor Method (IFM). The principal inconvenience of the t-z method arises from the determination of the resisting curve's shape; an improvement upon this aspect is the main aim of this study. Partial slip is considered using a new analytical approach which is an adaptation of a model based on bond degradation. Pile installation effects and interface strength reduction are uncoupled and considered explicitly in this study. Lateral profiles of mean effective stress after pile installation and subsequent consolidation which were representative of predictions determined in a previous study using a modified version of the cavity expansion method (CEM) are adopted; these predictions are subsequently used to relate installation effects to changes in soil strength and stiffness. In addition, the ‘reinforcing’ effects of a second, ‘receiver’, pile on the free-field soil settlement is considered using a nonlinear iterative approach where the relative pile-soil settlement along the pile shaft is related to the soil spring stiffness. Through comparisons with previously published field test data and numerical simulations, the results indicate that the proposed approach provides a sufficiently accurate representation of pile behaviour while conserving considerable computing requirements.

Keywords: settlement, pile interaction, pile groups, nonlinear, analytical

33 1. Introduction

34 The topic of single pile and pile group behaviour under vertical load has been covered
35 extensively in the literature over the past few decades. This has lead to the employment of
36 numerous rigorous methods to consider the pile-soil system as one composite continuum
37 including the boundary element method (e.g. Basile [1] and the finite element (FE) method
38 (e.g. Sheil and McCabe [2]) These numerical methods are regarded as some of the most
39 robust approaches to single pile and pile group analysis and can take into account various
40 complex factors such as soil anisotropy, constitutive modelling, pile-soil-pile interaction and
41 complex 3-dimensional group geometries. A limitation to these continuum analyses,
42 however, is that considerable numerical expertise and computational resources are required
43 for the analysis of the entire pile-soil system.

44 Simplified analytical approaches have the advantage over rigorous continuum analyses in that
45 a designer can obtain an estimate of pile settlement quite quickly and without the need of the
46 computing requirements associated with rigorous continuum analyses. Moreover, they may
47 often prove the only feasible analysis for larger group sizes with non-standard geometries.
48 The load transfer (t-z) method was first proposed by Seed and Reese [3] and has since been
49 considered by numerous investigators to describe the linear elastic (LE) load-displacement
50 relationship of a single pile [4-6]. These methods were later advanced by Mylonakis and
51 Gazetas [7] to take account of the ‘reinforcing’ effects of a pile on the soil continuum for the
52 prediction of two-pile interaction factors.

53 The concept of considering soil nonlinearity through the use of hyperbolic load-transfer
54 functions, first documented by Kraft *et al.* [8], has since been adopted by numerous
55 investigators, e.g. [9-13]. Wang *et al.* [14] improved upon these methods by using an iterative
56 approach to incorporate the degradation in stiffness of the concrete pile under compressive
57 loads using the well-documented nonlinear Hognestad model [15].

58 While the aforementioned approaches have advanced simplified single pile and pile group
59 analysis, there are various limitations associated with each. One such limitation is the
60 assumption of pre-failure perfect pile-soil bonding. Even at low load levels, the development
61 of slippage at the contact between pile and soil (defined herein as ‘partial slip’) is a likely
62 phenomenon [16, 17]. Trochanis et al. [18] also reported the importance of pile-soil slip with
63 regard to the load-displacement response of a single vertically loaded pile and two-pile

interaction factors. Similarly, Perri [19] noted that one of the main differences between a simple shear test and the soil surrounding an axially loaded pile is the possibility of slip occurring between the pile and the adjacent soil element. Furthermore, while Mylonakis and Gazetas [7] considered pile ‘reinforcing’ effects in a LE soil medium, a similar approach has not been implemented in recent nonlinear analytical models nor have the effects of soil disturbance arising from pile installation been considered explicitly.

In this paper, the ‘t-z method’ is employed to describe the nonlinear behaviour of a single pile and is used to obtain predictions of pile group behaviour by considering the interaction between two-piles in conjunction with the Interaction Factor Method (IFM). The principal inconvenience of the t-z method arises from the determination of the resisting curve's shape; an improvement upon this aspect is the main aim of this study. Partial slip is considered using a new simplified approach which is an adaptation of the bond degradation model first proposed by Gens and Nova [20]. Using this method the degradation of bonds, due to particle re-orientation and the remoulding of the structure to eventually a residual state within the clay shear band surrounding the pile, is related to the amount of slip at the pile-soil interface. The ‘initial stress technique’ [21] is used to consider full pile-soil slip occurring at limiting shear stress.

Although undrained conditions are assumed, in contrast to the α -method of pile capacity design first proposed by Tomlinson [22], pile installation effects and interface strength reduction are uncoupled and considered explicitly in this study. In a previous study conducted by Sheil *et al.* [23] the FE software package PLAXIS 2-D in conjunction with the MIT-S1 constitutive model was adopted to model pile installation effects using a modified Cavity Expansion Method (CEM) in two well-investigated soils, namely San Francisco Young Bay Mud (YBM) and Boston Blue Clay (BBC). The predictions of the permanent change in mean effective stress around an installed pile obtained from that study have been adopted herein to relate long-term stress changes to changes in both the strength and stiffness of the surrounding soil. In addition, the ‘reinforcing’ effects of a second, ‘receiver’, pile on the free-field soil settlement is considered using a nonlinear iterative approach where the relative pile-soil settlement along the pile shaft is related to the soil spring stiffness. The present approach is validated against three well-documented case histories.

2. Soil nonlinearity

The relationship proposed by Randolph and Wroth [24] has been employed to predict the reduction of shear stress with radial distance from the pile which can be defined as follows:

$$\tau_{soil} = \tau_i \left(\frac{R}{r} \right) \quad (1)$$

where τ_i is the shear stress in the soil at the pile-soil interface, τ_{soil} is the shear stress in the soil at a radial distance r from the pile's vertical axis of symmetry and R is the pile radius or equivalent pile radius (if non-circular).

The vertical displacements of the soil at a particular point surrounding the pile are then obtained by integrating the shear strains (γ) from that location outwards to a value of $r = r_m$:

$$w = \int_r^{r_m} \gamma dr = \sum_r^{r_m} \gamma \Delta r \quad (2)$$

where $\gamma = \tau / G_{sec}$, G_{sec} is the secant shear modulus and τ is the shear stress. The value of r_m , defined by Randolph and Wroth [24] as the radius at which the shear stress in the soil becomes negligible, was conservatively chosen as $200R$. Soil displacements at the pile-soil interface are thus obtained by integrating the shear strains from a distance r_m to a distance R .

For the nonlinear predictions, the relationship proposed by Lee and Salgado [25] was adopted defined as:

$$G_{sec} = G_0 \left(1 - f \left(\frac{\tau}{\tau_f} \right)^g \right) \left(\frac{p'}{p_0'} \right)^n \quad (3)$$

where f and g are empirical curve fitting parameters, p' is the mean effective stress which has a far field value of p_0' , n is a constant between 0.5 and 1 and controls the stress dependency of soil stiffness, τ is the shear stress at a particular radial distance, r , from the pile and τ_f is the shear stress at failure. For pile loading in clays, undrained conditions are assumed; therefore the shear stress at failure can be defined as:

$$\tau_f = \frac{s_u}{2} \quad (4)$$

where s_u is the undrained shear strength of the soil.

At the pile-soil interface, however, the shear strength between pile and soil is often substantially less than the shear strength of the soil mass. In this study, reference is made to the databases reported by Potyondy [26] and Tiwari *et al.* [27] for the selection of an interface strength reduction factor, R_{inter} , such that:

$$s_{u,i} = R_{inter} s_{u,soil} \quad (5)$$

where $s_{u,i}$ is the undrained shear strength at the pile-soil interface and $s_{u,soil}$ is the undrained shear strength of the soil mass. Therefore, the limiting shear stress that can be maintained at the pile-soil interface corresponds to $0.5*s_{u,i}$.

The base load-displacement relationship is calculated using the hyperbolic model proposed by Guo and Randolph [13] defined as:

$$w_B = \frac{P_B(1-\nu_s)\omega}{4RG_{iB}} \frac{1}{\left(1 - R_{fB} \frac{P_B}{P_{Bu}}\right)^2} \quad (6)$$

where w_B is the pile base settlement; P_B is the pile base load; ν_s is the Poisson's ratio of the soil; G_{iB} is the shear modulus at the pile base; ω is the pile base shape and depth factor which is often set equal to 1 [6, 24]; P_{Bu} is the limiting base load; and R_{fB} is a parameter that determines the extent of soil nonlinearity. Assuming undrained conditions, the parameter P_{Bu} can be estimated as follows:

$$P_{Bu} = N_c s_u A_b \quad (7)$$

where N_c is the bearing capacity factor, taken as 9, s_u is the undrained shear strength at the pile base and A_b is the area of the pile base.

3. Pile-soil slip

3.1. Shear bands in clay

Numerous studies have reported that for clays, the soil within the shear band undergoes significant particle re-orientation and is eventually remoulded into a residual state [28]. While research on shear bands in sands has identified significant correlations between shear band thicknesses, t_s , and the mean grain size, d_{50} , shear band thicknesses in clays cannot be correlated to grain size so readily, however [29]. While values of t_s for clays reported in the literature vary from 1.4 – 20 mm, Vardoulakis [30] recommended a conservative value of $t_s = 200d_{50}$; this value gave the best fit to the data presented later in the paper.

3.2. Partial slip

In the present study, the authors differentiate 'partial slip' occurring at working stresses ($\tau_i < \tau_f$) from 'full slip' when $\tau_i = \tau_f$. As mentioned, while most numerical methods can now account for partial pile-soil slip by introducing interface elements into the model, existing

simplified analytical methods have assumed ‘pre-failure’ perfect pile-soil bonding i.e. no partial slip.

In this section, a new analytical approach is proposed to consider partial pile-soil slip at the interface by considering the bond degradation within the aforementioned shear band surrounding the pile-soil interface. Bond degradation occurs when the inter-particle bonds are progressively destroyed by inter-particle shear and normal displacements. The bond degradation model was first proposed by Gens and Nova [20] where the amount of particle bonding is described with a scalar state variable χ , which is changing (ultimately to zero) due to bond degradation and is defined as:

$$d\chi = -\xi \cdot \chi \cdot (|d\varepsilon_v^p| + \xi_d \cdot |d\varepsilon_d^p|) \quad (8)$$

where $d\chi$ is the rate of bond degradation; ξ is the absolute rate of bond degradation; ξ_d is the relative rate of bond degradation; $d\varepsilon_v^p$ is the rate of plastic volumetric straining and $d\varepsilon_d^p$ is the rate of plastic deviatoric straining.

This logic was adopted in the rotational hardening elasto-plastic S-CLAY1S model described by Koskinen *et al.* [31] to describe destructuration with progressive plastic straining.

The rate of plastic volumetric strain, $d\varepsilon_v^p$, is defined as:

$$d\varepsilon_v^p = d\varepsilon_{11}^p + d\varepsilon_{22}^p + d\varepsilon_{33}^p \quad (9)$$

while the rate of plastic deviatoric strain, $d\varepsilon_d^p$, is defined as:

$$d\varepsilon_d^p = d\varepsilon_{11}^p - d\varepsilon_{33}^p \quad (10)$$

During pile loading it is assumed that $d\varepsilon_{11}^p \gg d\varepsilon_{33}^p, d\varepsilon_{22}^p$; thus for the case of simple shear Eq. 8 reduces to:

$$d\chi \approx -2 \cdot |d\gamma^p| \cdot \xi \cdot \chi \cdot (1 + \xi_d) \quad (11)$$

where $d\gamma^p$ is the rate of plastic shear strain and γ^p is defined herein as:

$$\gamma^p = \tau \left(\frac{1}{G_{sec}} - \frac{1}{G_0} \right) \quad (12)$$

The current amount of bonding can thus be deduced by using the following equation:

$$\chi = \chi_0 + d\chi \quad (13)$$

where χ_0 is the initial amount of bonding and can be determined from the soil sensitivity, S_r , as follows [32]:

$$\chi_0 = S_r - 1 \quad (14)$$

There is currently little guidance in the literature on appropriate values of ξ and ξ_d for different soil types. Values of ξ and ξ_d have been reported by Yin and Karstunen [32] as being typically in the relatively narrow range of 8 to 12 and 0.2 to 0.3, respectively; in the present study a value of 10 and 0.25 have been chosen for ξ and ξ_d , respectively. Further studies on bond degradation are required to investigate the dependence of bond degradation rates on χ_0 .

From field tests, Broms [33] reported typical measurements of limiting pile-soil relative shear displacement (γ_{crit}) in the range of 1-8 mm; an average value of 5 mm has been assumed by numerous authors in the literature since, e.g. Lee *et al.* [34], and has also been adopted herein. In these studies, once the relative shear displacement at the pile-soil interface reaches γ_{crit} , the shear stiffness at the pile-soil interface becomes zero. In this study, γ_{crit} has been chosen to correspond to complete bond degradation i.e. $\chi = 0$. In addition, the authors have assumed the magnitude of partial slip between pile and soil to be linearly related to the strength of the bond between them and thus propose the following relationship for the determination of w_{slip} :

$$w_{slip} = \gamma_{crit} \left[\frac{-d\chi}{\chi_0} \right] \quad (15)$$

Unfortunately, prediction of the slip at the pile-soil interface under working loads has not been researched to date. While there is a certain degree of speculation in the selection of this relationship, the authors believe this is a logical first step in relating pile-soil slip to soil properties. The value of $d\chi$ used in Eq. 15 is the average value within the shear band annulus described in Section 3.1.

3.3. Full slip

Shen and Teh [35] employed an ‘initial stress technique’ in order to consider ‘full slip’ in the case of downdrag forces on pile groups and this method has also been adopted here. This involves an iterative procedure where a limiting value of $\tau_{f,i}$ is imposed on the shear stresses at the pile shaft, τ_i , and excess soil shear stresses are redistributed to areas along the piles shaft where $\tau_i < \tau_{f,i}$. This usually involves redistributing stresses further down the pile where $\tau_{f,i}$ is higher due to higher confining stresses.

4. Pile installation effects

4.1. Single pile effects

Permanent changes to the effective stress regime in the soil due to pile installation are difficult to consider in any analytical approach due to the high 2-dimensional gradients, large deformations and complex soil behaviour associated with soil disturbance effects. Sheil *et al.* [23] conducted a comprehensive FE study of driven pile installation effects in clay using a variation on the traditional cavity expansion method (CEM) where vertical displacements were imposed concurrently with the expansion of the cavity; the strain-softening MIT-S1 constitutive model was employed as a user-defined soil model in PLAXIS 2D for this purpose. Arising from that study, Fig. 1 presents a simplified model adopted herein to consider the influence of pile installation. The trends are representative of the predicted distribution of normalised mean effective stress after single pile installation and subsequent consolidation versus normalised radial distance where the overconsolidation ratio (OCR) was varied between 1 and 4 [23]. Furthermore, those authors noted that predictions of mean effective stress increases after installation and consolidation for both very soft San Francisco Young Bay Mud and stiff Boston Blue Clay were similar; therefore these results are considered independent of the soil type. Further information is provided elsewhere [23].

A number of authors have represented undrained shear strength by the normalised value (s_u/p'), where p' is current mean effective stress e.g. Amerasinghe and Parry [36]. Thus in the present study, the undrained shear strength of soil in the vicinity of a single pile after consolidation is modified as follows:

$$s_{u(r)} = s_{u,0} \left(\frac{p'(r)}{p'_0} \right) \quad (16)$$

where $s_{u(r)}$ is the undrained strength at a particular radial distance from the pile, $s_{u,0}$ is the undisturbed (far-field) undrained shear strength and the variation of p'/p'_0 with normalised radial distance is obtained from Fig. 1. Similarly, the influence of pile installation on soil stiffness can also be considered by incorporating the variation of p'/p'_0 in Eq. 3.

4.2. Pile group effects

Sheil *et al.* [23] also investigated the influence of additional group pile installations over-and-above the effects of single pile installation using PLAXIS 2D in conjunction with the extensively-employed Modified Cam-Clay model. The term ‘group installation effects’ is used in this paper to denote differences between the effective stress regime surrounding a (driven) group pile compared to an equivalent (driven) single pile.

It was shown that after the installation of a pile, the installation of additional neighbouring piles do not induce a further increase in the excess pore pressures near the pile-soil interface (i.e. in this case additional ‘group effects’ are negligible). Furthermore, after full consolidation all additional group effects diminished i.e. the effective stress regime in the vicinity of a group pile after installation and subsequent consolidation was similar to that of an equivalent single pile after installation and consolidation. This supported the findings of McCabe [37] who noted that the stress regime surrounding a driven 5-pile group installed in clay were similar to that surrounding a driven single pile at the same site. In light of these results, only the effects associated with each pile’s own installation has been dealt with in this study while any additional effects due to the installation of neighbouring piles has not been accounted for.

5. Concrete modulus degradation

While elastic pile compression has been adopted by numerous authors in the literature and can be considered acceptable for low load levels, longer piles with higher applied loads, however, can exhibit noticeable plastic deformation [14]. Thus the nonlinear Hognestad model [15] was adopted in the present study to describe the stress-strain relationship of the concrete pile as follows:

$$\sigma_c = \begin{cases} f_c \left[2 \frac{\varepsilon_c}{\varepsilon_0} - \left(\frac{\varepsilon_c}{\varepsilon_0} \right)^2 \right] & \{\varepsilon_c \leq \varepsilon_0\} \\ f_c \left[1 - 0.15 \left(\frac{\varepsilon_c - \varepsilon_0}{\varepsilon_{cu} - \varepsilon_0} \right)^2 \right] & \{\varepsilon_0 < \varepsilon_c \leq \varepsilon_{cu}\} \end{cases} \quad (17)$$

where σ_c and ε_c are the current stress and strain of concrete, respectively; f_c and ε_0 are the peak stress and corresponding strain, respectively; and ε_{cu} is the ultimate strain of the concrete (see Fig. 2). Since strains in the range $\varepsilon_c \leq \varepsilon_0$ are under consideration, the Young’s modulus of the concrete can be obtained using the expression:

$$E_c = \frac{2f_c}{\varepsilon_0^2} (\varepsilon_0 - \varepsilon_c) \quad (18)$$

In the present study, typical values of 30 MPa and 0.002 for f_c and ε_0 , respectively, have been adopted.

6. Iterative process for a single loaded pile: segment-by-segment method

The stress-dependency of soil stiffness is taken into account using the segment-by-segment method (SSM) proposed by Ghazavi [38]. In order to consider an increasing soil stiffness profile with depth, the pile is divided into n segments with length h as shown in Fig. 3; a value of $h=0.5$ m was selected as the optimum segment length for the case histories considered in the present paper.

A flow chart of the present approach is provided in Fig. 4 and described below:

1. A value of pile base load, P_{BI} , is selected.
2. The pile base settlement, w_{BI} , is obtained from the hyperbolic relationship defined in Eq. 6.
3. From P_{BI} the settlement at the top of segment n , $(w_{11})_{n1}$, is calculated as:

$$(w_{11})_{n1} = w_{BI} + w_c \quad (19)$$

where w_c is the pile compression and can be calculated as:

$$w_c = \left(\frac{(P_{11})_{n1} + (P_{11})_{n2}}{2} \right) \left(\frac{h}{EA} \right) \quad (20)$$

where $(P_{11})_{n1}$ and $(P_{11})_{n2}$ are the forces at the top and bottom, respectively, of segment n of pile 1 due to its own externally applied load. For a concrete pile, the value of E should be obtained using Eqs. 17 and 18.

4. The settlement at the midpoint of segment n is then used to obtain the corresponding local shear stress for segment n , $\tau_{n,r=R}$, from Eqs. 1-3.
5. The value of $(P_{11})_{n1}$ is then calculated as:

$$(P_{11})_{n1} = P_{BI} + 2\pi R(\tau_{n,r=R}).h \quad (21)$$

6. Steps 3-5 are repeated for segments $n-1$ to 1 where $(P_{11})_{j1} = (P_{11})_{(j-1)2}$.
7. The values of P_{TI} and w_{TI} corresponding to the selected value of P_{BI} in step 1 are obtained.
8. Steps 1-7 are repeated for different values of P_{BI} to obtain the load-displacement response.

7. Extension to group behaviour

7.1. Pile shaft 'interactive' displacements

For the extension of the present method to the analysis of a pile group, the Interaction Factor Method (IFM) has been adopted. McCabe and Sheil [39] conducted a study on the appropriate use of two-pile nonlinear interaction factors in pile group analysis. Those authors identified two different methods for the prediction of two-pile interaction factors, namely

Approach I where the ‘receiver’ pile is loaded and Approach II where the receiver pile is non-loaded and concluded that Approach II was the most appropriate method for the settlement estimation of pile groups where the two-pile interaction factor, α is defined as:

$$\alpha = \frac{w_{21}}{w_{11}} \quad (22)$$

where w_{11} is the settlement of pile 1 under its own load and w_{21} is the settlement of a nearby non-loaded pile 2 at a spacing of s/D .

The additional ‘interactive’ displacements between pile shafts are obtained by integrating the shear strains from the radial distance between the loaded single pile and the receiver pile to a radial distance equal to r_m using Eq. 2; this process is repeated at the level of each segment along the length of the pile. Additional details of this approach are provided in Section 7.3. While floating pile groups are considered herein, this process may be applied to end-bearing pile groups through the use of modified value of r_m .

7.2. Pile base ‘interactive’ displacements

In addition to pile shaft interaction, a displacement field is also generated beneath the pile base. In this study, interaction between pile shafts and pile bases are assumed to be uncoupled. Additional pile base ‘interactive’ displacements are determined using the solution for a rigid punch on an elastic half-space proposed by Randolph and Wroth [40] defined as:

$$(w_{21})_B = w_{B1} \frac{2}{\pi} \left(\frac{R}{r} \right) \quad (23)$$

where $(w_{21})_B$ is the additional interactive base displacements due to the base displacements of a nearby loaded pile 1 i.e. w_{B1} . The total displacements at the base of the receiver pile can then be obtained as follows:

$$w_{B2} = (w_{21})_B + (w_{22})_B \quad (24)$$

where $(w_{22})_B$ is the displacement at the base of pile 2 due to the imposed vertical load within the pile and w_{B2} is the total base settlement of the receiver pile.

7.3. Receiver pile ‘reinforcing’ effects

A non-loaded ‘receiver’ pile placed within the displacement field of the source pile will not exactly follow the free-field soil settlement due to the axial stiffness of the pile and

interaction with the surrounding soil [7]; differences between the settlement of a non-loaded ‘receiver’ pile and the free-field soil displacements is referred to as ‘reinforcing effects’ herein. Mylonakis and Gazetas [7] originally identified the ‘reinforcing’ effects of a non-loaded ‘receiver’ pile on free-field displacements ($U_{r,z}$) while Ghazavi [38] later extended this approach to account for a layered soil profile using the ‘segment by segment method’ (SSM).

In this study, the SSM has been adopted in a similar manner as adopted for the analysis of a single pile described in Section 6 in order to take account of soil stiffness nonlinearity. Both piles are divided into an equal number of segments with equal thickness h where each layer is assumed to have the same soil properties, although it is also possible to consider a lateral variation in soil properties in a spreadsheet format. Each segment is then analysed as a full pile with the length of the pile being equal to the thickness of the soil layer [38].

In the present study, while interaction effects are assumed uncoupled, pile shaft resistance and the load-displacement relationship at the pile base are coupled, thus a new ‘trial and error’ approach must be adopted as follows:

1. A vertical load is applied at the head of the ‘source’ pile (see Fig. 5) and the variation of w_{11} with depth is calculated using the approach outlined in Section 6.
2. The free-field soil settlement at the location of the non-loaded pile (at $r = r_2$) and depth z (i.e. $U_s(z)$) can be calculated by integrating the shear strains from a distance r_m to a distance r_2 using Eq. 2, where r_2 is the radial distance to the location of the receiver pile.
3. An arbitrary value close to P_{B1} is chosen for the force at the base of the receiver pile, P_{B2} .
4. The value of $(w_{22})_B$ is calculated using the hyperbolic relationship defined by Eq. 6.
5. The value of w_{B2} can then be obtained using Eqs. 23 and 24.
6. The compression of segment n under P_{B2} is calculated using Eq. 20 and $(w_{21})_{n1}$ can be determined.
7. The relative pile-soil settlement (at depth z) can be obtained by subtracting the free-field soil displacement at the location of the receiver pile, $U_s(r,z)$, from the actual receiver pile settlement, $w_{21}(z)$. With the soil spring reaction, k_z , being dependent on the displacement of the pile relative to the free-field soil displacements, the vertical equilibrium of each pile segment can be expressed as follows [7]:

$$E_p A_p \frac{d^2 w_{21}(z)}{dz^2} - k_z [w_{21} - U_s(r, z)] = 0 \quad (25)$$

where $U_s(r, z)$ has been obtained in step 2; $w_{21}(z) - U_s(r, z)$ is the relative pile-soil settlement; E_p is the Young's modulus of the pile; A_p is the cross-sectional area of the pile; k_z is the nonlinear soil spring stiffness defined as:

$$k = \delta \cdot G_{sec} \quad (26)$$

where $\delta = \ln \frac{2\pi}{(r_m/R)}$ and G_{sec} is obtained from the nonlinear relationship in Eq. 10.

8. The value of $(P_{21})_{n1}$ can be obtained as follows:

$$(P_{21})_{n1} = P_{B2} - (2\pi R h) E_p A_p \frac{d^2 w_{21}(z)}{dz^2} \quad (27)$$

where the value of E_p should be obtained using Eqs. 17 and 18 for a concrete pile.

9. Steps 5-7 are repeated for segments $n-1$ to 1 where $(P_{21})_{j1} = (P_{21})_{(j-1)2}$

10. The force and settlement at the head of the receiver pile, P_{T2} and w_{T2} , respectively, are calculated using the iterative process above.

11. Since the receiver is *non-loaded*, if the computed value of $P_{T2} = 0$ then the corresponding computed value of w_{T2} is correct. If $P_{T2} \neq 0$ the assumed value of P_{B2} must be refined in the next trial.

8. Validation

8.1. Case I: FE analyses of a single pile at Hutton

A summary of the required input parameters for the present approach, in addition to their physical meaning and selected values for each case study is presented in Table 1. Jardine and Potts [41] described the FE analysis of a single pile and 8-pile group at the well-documented Hutton tension leg platforms which was carried out in parallel with the field monitoring program at the same site [42]. Results of the site investigation were supplemented with measured data for Magnus clay from a nearby site; the properties of Magnus clay were deemed to represent a suitable basis for the estimation of other nearby low plasticity tills [43]. Only the analysis of the single pile is considered in the present study since the eccentric tension loading of the 8-pile group also induced moment rotation which is outside the scope of the present paper. The FE analysis was carried out using the Modified Cam-Clay model to

simulate the Hutton clay while the Mohr-Coulomb model was deemed sufficient to model intermediate sand lenses. The steel pile was modelled as a solid elastic cylinder with a diameter, D , of 1.83 m and an equivalent Young's modulus of 28 GPa.

Values of the initial elastic shear modulus G_0 were obtained from the vertical profile of small-strain Young's modulus reported by Jardine [44] for Magnus clay (using $\nu = 0.5$ for undrained conditions). Values of f and g equal to 0.9 and 0.6, respectively, were chosen by calibrating predictions to measured shear modulus degradation curves in triaxial compression documented by Jardine and Potts [41] (see Fig. 6) where values of G_{sec} were again calculated from E_{sec} with $\nu = 0.5$. The variation in s_u with depth was obtained from Jardine and Potts [41] which varied in the range 200 ± 50 kPa.

In this study, reference was made to the database of interface strength reduction factors documented by Potyondy [26] where a value of $R_{inter} = 0.3$ was chosen for the clay-smooth steel interface in undrained conditions. Values of OCR with depth were chosen based on those documented for the Magnus clay site by Jardine [44] and Jardine and Potts [45] which were typically 10 ± 5 for depths between 0 m to 20 m, 3 ± 1 for depths between 20 m to 40 m and was approximately equal to 1 for depths greater than 40 m; these values were subsequently used to derive the corresponding distribution of mean effective stress due to pile installation effects from Fig. 1. As mentioned, however, the numerical study of installation effects was limited to an OCR of 4 thus higher OCRs were limited to the results for OCR=4.

A value of $S_r = 2.6$ was calculated based on the measured undrained shear strengths in triaxial compression on reconstituted Magnus clay reported by Jardine and Potts [45]. A value of d_{50} of 7.5×10^{-4} mm was selected based on physical measurements of Magnus clay [46]; the thickness of the shear band, t_s , surrounding the pile was then calculated as $200d_{50}$. The shear strain within the shear band was employed to obtain the magnitude of partial slip at the interface of the piles.

In Figs. 7a – 7c, predictions of load-transfer relationships determined by the present approach for a depth of 16 m, 28 m, and 47 m, respectively, have been compared to nonlinear FE predictions documented by Jardine and Potts [41] where the value of z was calculated as the pile head settlement less tension lengthening of the pile from the pile head to the level of interest. It can be seen for all three depths, both sets of predictions show good agreement.

Since the pile was loaded in tension, the load-displacement characteristics at the pile base are not considered. In Fig. 8, predictions of the single pile load-displacement relationship

determined by the present approach and FE analyses have been compared where results also show good agreement.

8.2. Case II: single pile and 5-pile group load tests in soft estuarine silt

The pile load test programme documented by McCabe [37] consisted of a single pile and 5-pile group installed in soft Belfast clay known locally as ‘*sleech*’. Precast square concrete piles with an equivalent diameter, D_{eq} , of 0.282 m were driven to a depth of 6 m. The group piles were arranged with a centre pile surrounded by four corner piles at a spacing-to-diameter (s/D_{eq}) ratio of 2.8.

The initial elastic shear modulus, G_0 , was chosen equal to 10 MPa based on seismic cone tests on the Belfast *sleech* which was relatively constant with depth [37]. The parameters f and g were back-calculated as 1.0 and 0.3, respectively from curve-fitting to the measured shear modulus degradation curve in triaxial compression documented by McCabe ([37]; see Fig. 9) where the secant shear stiffness values, G_{sec} , have been normalised by the initial mean effective stress at the beginning of undrained shearing, p'_0 (=30 kPa). Values of s_u were chosen based on the undrained shear strength profile reported in McCabe [37] where s_u varied between 20 ± 2 kPa.

A value of $R_{inter} = 0.55$ was adopted for the site-specific interface strength reduction for a *sleech*-concrete interface [47, 48]. Values of OCR were chosen based on the values reported by McCabe [37] which decreases from a value of 2 at a depth of 2 m to 1.2 at depths of ~3 m to 6 m.

Values of S_r for the Belfast test site were reported by McCabe [37] to vary between a value of 2 and 3. An average value of d_{50} equal to 0.015 mm was deduced from the values reported by Lehane [49] for depths ranging between 3.3 m to 6.65 m leading to a value of $t_s = 3$ mm.

Predictions of soil reaction curves determined by the present approach have been compared to measured data curves at 3.25 m and 5.23 m levels in Figs. 10a – 10b, respectively, where the value of w was calculated as the pile head settlement less compression shortening of the pile from the pile head to the level of interest. It can be seen that good agreement is observed between predictions and measured data in Figs. 10a. Discrepancies between predictions and measurements in Fig. 10b at 5.25 m are believed to be related to anomalous measurements when considered in conjunction with previously published site investigations in the literature [37, 49].

An ultimate pile base load, P_{Bu} , of 9 kN was calculated using Eq. 7 while the value of G_{bu} was chosen as 15 MPa [37, 49]. A value of 0.8 was chosen for R_{fb} by calibrating the present predictions of the base load-displacement relationship to the measured data documented by McCabe [37] as shown in Fig. 11.

In addition, the analysis of the single pile was extended to that of a 5-pile group using IFM approach outlined in Section 7. The predicted load-displacement of the 5-pile group by this method have been compared to the measured load-displacement response documented by McCabe [37] in Fig. 12. It can be seen from Figs. 10 - 12, that results determined by the present approach show good agreement to the measured load-displacement response for both a single pile and 5-pile group in Belfast *sleech* in addition to traditional two-pile interaction factors.

In order to discern the influence of various aspects of the present model, the model has been stripped back to its most basic form and each section added in stages; predictions of two-pile interaction factors have been used for this purpose (see Fig. 13). The dashed line represents the most basic predictions determined using this model i.e. a LE soil medium with no allowance for pile-soil slip (by setting the parameter f to 0), receiver pile reinforcing effects or installation effects. The influence of soil stiffness nonlinearity is obviously dependant on the adopted load level; a factor of safety on single pile capacity of 2.5 has been adopted in Fig. 13, where the pile capacity was defined nominally at a pile head displacement of $0.1D$. In addition, measured data from the Belfast test site [37] have also been superimposed on the plot; the range of these values represent the variation in interaction factors with load level.

It can be seen that present predictions show good agreement with LE prediction of two-pile interaction factors previously documented in the literature using the computer program *PIGLET* [50], which is to be expected. It is also clear that the final predictions (including all model aspects) show good agreement to the higher datapoints of the measured data (which would correspond to the same FOS).

8.3. Case III: single pile and 9-pile group load tests in stiff overconsolidated clay

O'Neill *et al.* [51] reported the results of a series of tests carried out on single piles and pile groups in stiff overconsolidated Houston clay. Nine of the piles were installed in a 3×3 group formation with a value of $s/D = 3$ and were connected to a rigid pile cap. The single piles were located at a distance of 3.7 m either side of the pile group. In addition, a 4-pile sub-

group was also loaded and is also considered. All piles had an external diameter of 274 mm, wall thickness of 9.3 mm and were driven to a depth of 13.1 m below ground level.

The Young's modulus of the steel pile was taken as $E_p = 210$ GPa. Values of G_0 were obtained from Chow [9] where values increased approximately linearly from 47.9 MPa at the ground surface to 151 MPa at the base of the piles. Shear modulus degradation parameters were determined by calibrating predictions to the measured stress-strain curve in UU triaxial compression documented by Dunnavant and O'Neill [52] where a values of f and g equal to 0.95 and 0.35, respectively, were selected (see Fig. 14).

The profile of s_u with depth was obtained from O'Neill *et al.* [53] and Dunnavant and O'Neill [52] which varied with depth from a value of ~ 50 kPa at the ground surface to ~ 200 kPa near the base of the piles. A value of $R_{inter} = 0.3$ was again chosen for the clay-steel interface [26]. The OCR profile was obtained from O'Neill *et al.* [53] which varied from values of up to 8 at shallow depths to ~ 4 at depths > 9 m.

Dunnavant and O'Neill [52] reported values of d_{50} ranging between 1×10^{-2} mm and 7×10^{-2} mm. There was little guidance in the literature on the sensitivity of the clay at this test site; Heydinger and O'Neill [54], however, described the test site as "insensitive" and so a value of $S_r = 1$ has been adopted. A value of $S_r = 1$ in the present approach (i.e. a value of $\chi_0 = 0$) indicates that the value of w_{slip} is ill-defined, i.e. no partial pile-soil slip; while there is no validation for this in the literature, predictions of soil reaction curves for depths of 1 m – 2.5 m, 4 m – 7 m, 9 m and 10 m – 12 m determined by the present approach show reasonably good agreement to the measured data documented by O'Neill *et al.* [51] in Figs. 15a -15d, respectively. An increase in partial slip would lead to a more pronounced difference in results.

The ultimate end bearing capacity P_{Bu} was taken as 130 kN [11] while the initial soil stiffness at the pile base G_{iB} was taken as 150 MPa based on the shear modulus profiles documented by Chow [9]. A default value of $R_{fb} = 0.9$ yields good agreement between predictions and the measured base load-displacement response [51] in Fig. 16. In Fig. 17, the analysis of the single pile was extended to a 9-pile group and 4-pile group where predictions have again been compared to measured data documented by O'Neill *et al.* [51]. It can be seen that for both the single pile in Fig. 16 and the 4-pile and 9-pile groups in Fig. 17, predictions show good agreement to the measured data.

8.4. Case IV: Single pile and 4-pile group in soft Bangkok clay

The full-scale load tests of a single pile and a 4-pile group, with a value of $s/D=2.5$, documented by Brand *et al.* [55] has also been predicted here. All piles had a diameter of 150 mm and length of 6 m and were made of teak. The Young's modulus of the teak piles was taken as 10 Gpa based on typical values for timber piles documented by the American Forest and Paper Association [56]. A value of $R_{inter} = 0.5$ was chosen for the timber-clay interface [26]. Values of elastic shear modulus, G_0 , for Bangkok clay were obtained from seismic CPT results documented by Shibuya and Tamrakar [57] which varied between 12.5 ± 2 MPa from a depth of 2 m to ~10 m. Shear modulus degradation parameters were determined by calibrating present predictions to shear modulus degradation curves documented by Shibuya and Tamrakar [57] where values of f and g equal to 0.95 and 0.45, respectively, were selected (see Fig. 18).

The profile of s_u with depth was obtained from measured field vane values reported by Moh *et al.* [58] which varied in the range 15 ± 5 kPa between depths of 2 m to 10 m. A value of d_{50} of ~0.002 mm was chosen based on the grain size distribution documented by Tanaka *et al.* [59] for Bangkok clay. Brand *et al.* [55] reported an average value of S_r of 4 over the depth of interest while the OCR profile was taken from Moh *et al.* [58].

No information was given on the measured load-displacement at the base of the single pile load tests. The value of P_{Bu} was therefore estimated using Eq. 7 [60] where the value of s_u at the pile base was taken as 10 kPa [58]. A value of 12.5 MPa was selected for G_{ib} [59] while a default value of 0.9 was chosen for R_{fb} .

Single pile and pile group load-displacement predictions determined by the present study have been compared to measured data documented by Brand *et al.* [55] in Fig. 19. It can be seen from the figure that good agreement to the measured data is obtained using the present approach.

9. Conclusions

In this paper, an approach based on the 't-z method' has been presented to describe the nonlinear behaviour of a single pile where the interaction between two-piles in conjunction with the IFM has been employed to extend the approach to the analysis of pile groups. The majority of the input parameters in the formulated analytical solution have a physical

meaning and can be readily-obtained from independent traditional soil tests. The conclusions that can be drawn from the study are as follows:

- (a) Partial slip was considered using a new simplified approach which is an adaptation of the bond degradation model first proposed by Gens and Nova [37]. Using this method the degradation of bonds, due to particle re-orientation and the remoulding of the structure to eventually a residual state within the clay shear band surrounding the pile, is related to the amount of slip at the pile-soil interface.
- (b) Full pile-soil slip occurring at limiting shear stress is considered using the ‘initial stress technique’ similar to the approach employed by Shen and Teh [35] for the analysis of downdrag forces in pile groups.
- (c) Pile installation effects and interface strength reduction were uncoupled and considered explicitly. The authors adopted lateral profiles of mean effective stress after pile installation and subsequent consolidation which were representative of predictions determined by Sheil *et al.* [20] using a modified version of CEM. These predictions were used to relate installation effects to changes in soil strength and stiffness.
- (d) In addition, the ‘reinforcing’ effects of a second, ‘receiver’, pile on the free-field soil settlement was considered using a nonlinear iterative approach where the relative pile-soil settlement along the pile shaft is related to the soil spring stiffness.
- (e) Through comparisons with previously published field test data and numerical simulations, the results indicate that the proposed approach provides a sufficiently accurate representation of pile behaviour while conserving considerable computing requirements.

References

- [1] Basile F. Analysis and design of pile groups. In: Bull, editor. Numerical Analysis and Modelling in Geomechanics. London2003. p. 278-315.
- [2] Sheil BB, McCabe BA. Numerical modelling of pile foundation angular distortion. Soil Found. 2015;55(3):614-25.
- [3] Seed HB, Reese LC. The action of soft clay along friction piles. Transactions of the ASCE. 1957;122(731-54.
- [4] Coyle HM, Reese LC. Load transfer for axially loaded piles in clay. Journal of the Soil Mechanics and Foundations Division, ASCE. 1966;92(2):1-26.
- [5] Kraft Jr LM, Ray RP, Kagawa T. Theoretical t-z curves. Journal of the geotechnical engineering division. 1981;107(11):1543-61.
- [6] Armaleh S, Desai CS. Load deformation response of axially loaded piles. Journal of the Geotechnical Engineering Division, ASCE. 1987;113(12):1483-99.

- [7] Mylonakis G, Gazetas G. Settlement and additional internal forces of grouped piles in layered soil. *Geotechnique*. 1998;48(1):55-72.
- [8] Kraft LM, Ray RP, Kagawa T. Theoretical t-z curves. *Journal of the Geotechnical Engineering Division, ASCE*. 1981;107(11):1543-61.
- [9] Chow YK. Analysis of vertically loaded pile groups. *International Journal for Numerical and Analytical Methods in Geomechanics*. 1986;10(1):59-72.
- [10] Lee K, Xiao Z. A simplified nonlinear approach for pile group settlement analysis in multilayered soils. *Canadian Geotechnical Journal*. 2001;38(5):1063-80.
- [11] Castelli F, Maugeri M. Simplified nonlinear analysis for settlement prediction of pile groups. *Journal of Geotechnical and Geoenvironmental Engineering, ASCE*. 2002;128(1):76-84.
- [12] Zhang Q-Q, Zhang Z-M, He J-Y. A simplified approach for settlement analysis of single pile and pile groups considering interaction between identical piles in multilayered soils. *Computers and Geotechnics*. 2010;37(969-76).
- [13] Guo WD, Randolph MF. Vertically loaded piles in non-homogeneous media. *International Journal for Numerical and Analytical Methods in Geomechanics*. 1997;21(8):507-32.
- [14] Wang Z, Xie X, Wang J. A new nonlinear method for vertical settlement prediction of a single pile and pile groups in layered soils. *Computers and Geotechnics*. 2012;45(0):118-26.
- [15] Hognestad E, Hanson NW, McHenry D. Concrete stress distribution in ultimate strength design. *ACI Journal*. 1955;52(4):455-80.
- [16] Nishi K, Esashi Y. Field measurement and prediction of negative skin friction in piles. *Numerical Models in Geomechanics. Zurich 1982*. p. 776-84.
- [17] Phamvan. Negative skin friction on driven piles in Bangkok subsoils [PhD Thesis]. Bangkok, Thailand: AIT, 1989.
- [18] Trochanis AM, Bielak J, Christiano P. Simplified model for analysis of one or two piles. *Journal of Geotechnical Engineering*. 1991;117(3):448-66.
- [19] Perri JF. Assessment of capacity and seismic demand on axially loaded piles in soft clayey deposits [Ph.D. Thesis]. CA: University of California, Berkeley, 2007.
- [20] Gens A, Nova R. Conceptual bases for a constitutive model for bonded soils and weak rocks. *Geotechnical Engineering of Hard Soils-Soft Rocks*. Rotterdam: Balkema, 1993. p. 485-94.
- [21] Smith IM. *Programming the Finite Element Method with Application to Geomechanics*: John Wiley & Sons, Inc., 1982.
- [22] Tomlinson MJ. The adhesion of piles driven in clay soils. *Proceedings of the 4th International Conference on Soil Mechanics and Foundation Engineering*. London 1957. p. 66-71.
- [23] Sheil BB, McCabe BA, Hunt CE, Pestana JM. A practical approach for the consideration of single pile and pile group installation effects in clay: numerical modelling. *Journal of Geoenvironmental Engineering Sciences*. 2015;2(119-42).
- [24] Randolph MF, Wroth CP. Analysis of deformation of vertically loaded piles. *Journal of the Geotechnical Engineering Division, ASCE*. 1978;104(12):1465-88.
- [25] Lee JH, Salgado R. Determination of pile base resistance in sands. *Journal of Geotechnical and Geoenvironmental Engineering, ASCE*. 1999;125(8):673-83.
- [26] Potyondy JG. Skin friction between various soils and construction materials. *Geotechnique*. 1961;11(4):339-53.
- [27] Tiwari B, Ajmera B, Kaya G. Shear strength reduction at soil structure interface. *Advances in Analysis, Modelling and Design*. Florida: ASCE, 2010.
- [28] Dudoignon P, Pantet A, Carrara L, Velde B. Macro-micro measurement of particle arrangement in sheared kaolinitic matrices. *Géotechnique*. 2001;51(6):493-9.

- [29] Chakraborty T, Salgado R, Basu P, Prezzi M. Shaft resistance of drilled shafts in clay. *Journal of Geotechnical and Geoenvironmental Engineering ASCE*. 2013;139(4):548-63.
- [30] Vardoulakis I. Steady shear and thermal run-away in clayey gouges. *International Journal of Solids and Structures*. 2002;39(13):3831-44.
- [31] Koskinen M, Karstunen M, Wheeler SJ. Modelling destructuration and anisotropy of a natural soft clay. In: Mestat P, editor. *Proc 5th European Conference on Numerical Methods in Geotechnical Engineering (NUMGE 2012)*. Paris: Presses de l'ENPC, 2002. p. 11-20.
- [32] Yin ZY, Karstunen M. Influence of anisotropy, Destructuration and viscosity on the behaviour of an embankment on soft clay. *Proceedings of the 12th International Conference of International Association for Computer Methods and Advances in Geomechanics (IACMAG)*. Goa, India2008. p. 4728-35.
- [33] Broms B. Negative skin friction. *Proceedings of the Sixth Asian Regional Conference on Soil Mechanics & Foundation Engineering*. Singapore1979. p. 41-75.
- [34] Lee CJ, Bolton MD, Al-Tabaa A. Numerical modelling of group effects on the distribution of dragloads in pile foundations. *Geotechnique*. 2002;52(5):323-35.
- [35] Shen WY, Teh CI. A variational solution for downdrag force analysis of pile groups. *International Journal of Geomechanics*. 2002;2(1):75-91.
- [36] Amerasinghe SF, Parry RGH. Anisotropy in heavily overconsolidated Kaolin. *Journal of the Geotechnical Engineering Division, ASCE*. 1975;101(No. GT12):1277-93.
- [37] McCabe BA. *Experimental Investigations of Driven Pile Group Behaviour in Belfast Soft Clay [PhD]: Trinity College, Dublin, 2002.*
- [38] Ghazavi M. Vertical vibration of deep foundations in layered deposits. *3rd International Seminar on Soil Mechanics and Geotechnical Engineering*. Tehran, Iran2002. p. 223-8.
- [39] McCabe BA, Sheil BB. Pile group settlement estimation: suitability of nonlinear interaction factors. *ASCE Int J Geomech*. 2015;15(3):04014056.
- [40] Randolph MF, Wroth CP. Analysis of the vertical deformation of pile groups. *Geotechnique*. 1979;29(4):423-39.
- [41] Jardine RJ, Potts DM. Hutton tension leg platform foundations: prediction of driven pile behaviour. *Geotechnique*. 1988;38(2):231-52.
- [42] Jardine RJ, Hight DW, McIntosh W. Hutton Tension Leg Platform foundations: measurement of pile axial load-displacement relations. *Géotechnique*. 1988;38(2):219-30.
- [43] Jardine RJ, Hight DW. Measurements of soil stiffness at the Snorre site. Report to Saga Petroleum by Geotechnical Consulting Group. 1986.
- [44] Jardine RJ. *Investigation of pile soil behaviour with special reference to the foundations of offshore structures [PhD Thesis]: Imperial College London, 1985.*
- [45] Jardine RJ, Potts DM. Magnus foundations: Soil properties and predictions of field behaviour. *Conference on Large Scale Pile Tests in Clay*. London: Thomas Telford, 1993.
- [46] Nadeau PH. The physical dimensions of fundamental clay particles. *Clay Minerals*. 1985;20(499-514).
- [47] Strick van Linschoten CJ. Driven pile capacity in organic clays, with particular reference to square piles in the Belfast sleet 2004.
- [48] Sheil BB, McCabe BA. A finite element based approach for predictions of rigid pile group stiffness efficiency in clays. *ACTA Geotechnica*. 2014;9(469-84).
- [49] Lehané BM. Vertically loaded shallow foundation on soft clayey silt. *Proceedings of the ICE - Geotechnical Engineering*. 2003;156(1):17-26.
- [50] Randolph MF. *PIGLET: Analysis and design of pile groups users' manual*. Perth, Australia2003.
- [51] O'Neill MW, Hawkins RA, Mahar LJ. Load transfer mechanisms in piles and pile groups. *Journal of the Geotechnical Engineering Division, ASCE*. 1982;108(GT12):1605-23.

- [52] Dunnavant TW, O'Neill MW. Experimental p-y model for submerged, stiff clay. *Journal of Geotechnical Engineering*. 1989;115(1):95-114.
- [53] O'Neill MW, Hawkins RA, Mahar LJ. Field Study of Pile Group Action. Rep No FHWA/Rd-81/002, Federal Highway Administration. Washington, D.C.1981.
- [54] Heydinger AG, O'Neill MW. Analysis of axial pile-soil interaction in clay. *Int J Num Anal Meth Geomech*. 1986;10(4):367-81.
- [55] Brand EW, Muktabhant C, Taechathummarak A. Load tests on small foundations in soft clay. *Proceedings on the Performance of Earth and Earth-Supported Structures: ASCE*, 1972. p. 903-28.
- [56] American Forest and Paper Association (AFPA). National design specification for wood construction. Washington DC: American Forest and Paper Association, 2005.
- [57] Shibuya S, Tamrakar SB. Engineering properties of Bangkok clay. In: Tan TS, Phoon KK, Hight DW, Leroueil S, editors. *Characterisation and engineering properties of Natural Soils*. Rotterdam, the Netherlands: AA Balkema, 2002. p. 645-92.
- [58] Moh ZC, Nelson JD, Brand EW. Strength and deformation behaviour of Bangkok clay. *Proceedings of the 7th International Conference on Soil Mechanics and Foundation Engineering*. Mexico City1969. p. 287-95.
- [59] Tanaka H, Locat J, Shibuya S, Soon TT, Shiwakoti DR. Characterization of Singapore, Bangkok, and Ariake clays. *Canadian Geotechnical Journal*. 2001;38(378-400).
- [60] Janbu N. Static bearing capacity of friction piles. *Proceedings of the 6th European Conference on Soil Mechanics and Foundation Engineering*1976. p. 479-88.

Table 1

Table 1 Summary of input parameters for present approach

Par.	Physical meaning	Parameter determination/default value	Adopted case values				Units
			I	II	III	IV	
R	Pile radius	-	915	141	137	75	mm
r_m	Radial distance from pile to zero shear stress	200R	183	28.2	27.4	15	m
G_0	Small-strain shear modulus profile	Bender element or in-situ seismic cone penetration testing	130-150	~10	47.9-151	10.5-14.5	MPa
f, g	Parameters controlling soil stiffness nonlinearity	Curve-fitting to measured elemental stress-strain relationship	0.9, 0.6	1.0, 0.3	0.95, 0.35	0.95, 0.45	-
n	Stress dependency of soil stiffness	1.0 for cohesive soils	1.0	1.0	1.0	1.0	-
R_{inter}	Interface strength reduction	Site-specific interface tests or selection from suitable database [21,22]	0.3	0.55	0.3	0.5	-
N_c	Undrained bearing capacity factor	Default=9.0	9.0	9.0	9.0	9.0	-
ν_s	Poisson's ratio of the soil	Default=0.5 for undrained conditions	0.5	0.5	0.5	0.5	-
R_{fB}	Nonlinearity of pile base load-displacement relationship	Curve-fitting to measured data or use of a default value of 0.9	0.9	0.8	0.9	0.9	-
d_{50}	Mean grain size	Particle size distribution test	0.75	15	40	2	μm
ξ	Absolute rate of bond degradation	Default=10	10	10	10	10	-
ξ_d	Relative rate of bond degradation	Default=0.25	0.25	0.25	0.25	0.25	-
S_r	Soil sensitivity	In-situ shear vane or elemental shear testing	2.6	2-3	1	4	-
OCR	Overconsolidation ratio profile with depth	Oedometer tests on undisturbed samples	2-10	1.2-2.0	4-8	1.0-10	-
E	Young's modulus of pile	Pile fabrication specification	210	30	210	10	GPa
s_u	Undrained shear strength	In-situ shear vane or elemental shear testing	150-200	18-22	50-200	10-20	kPa

Fig. 1

[Click here to download high resolution image](#)

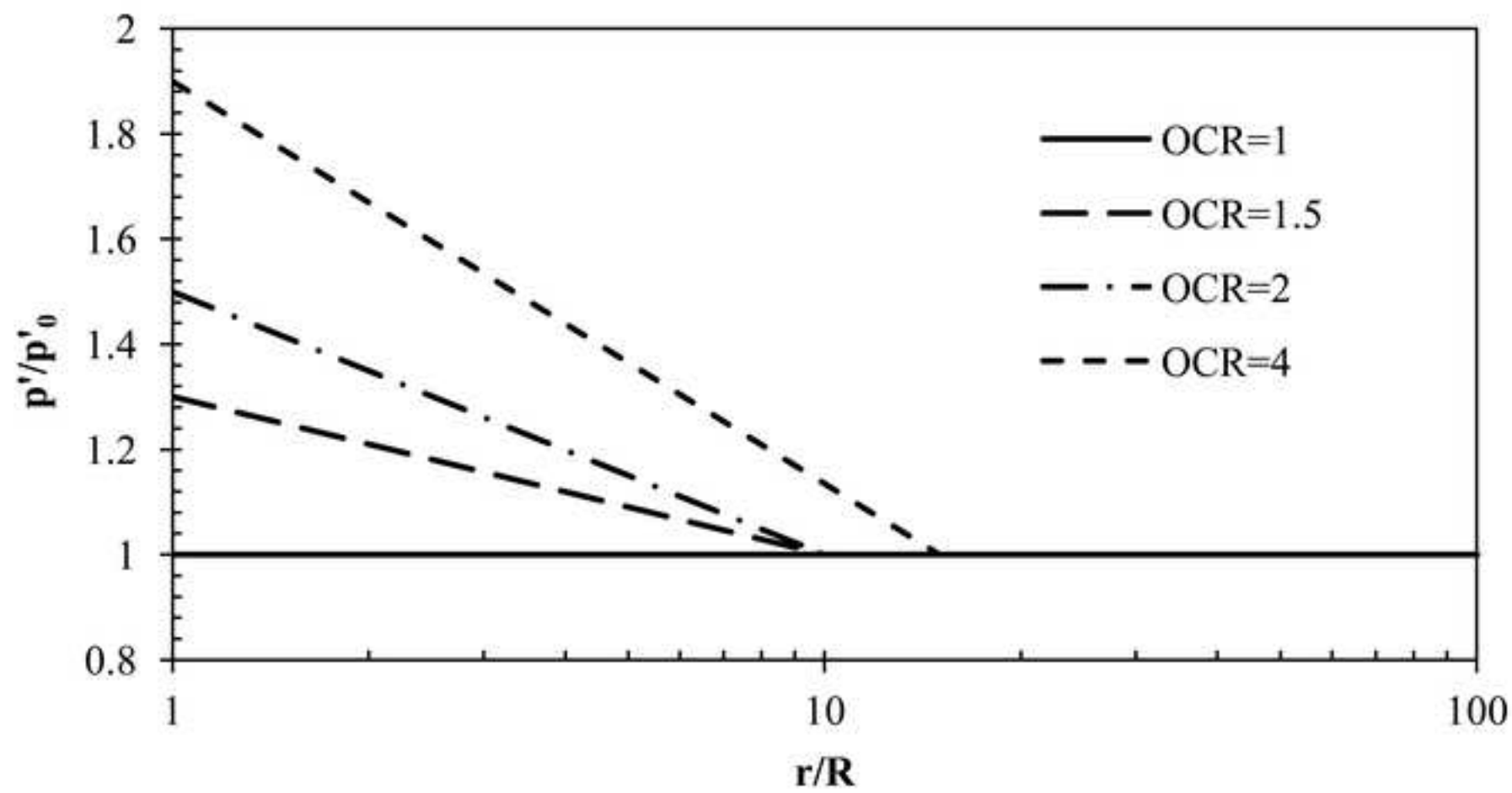


Fig. 2
[Click here to download high resolution image](#)

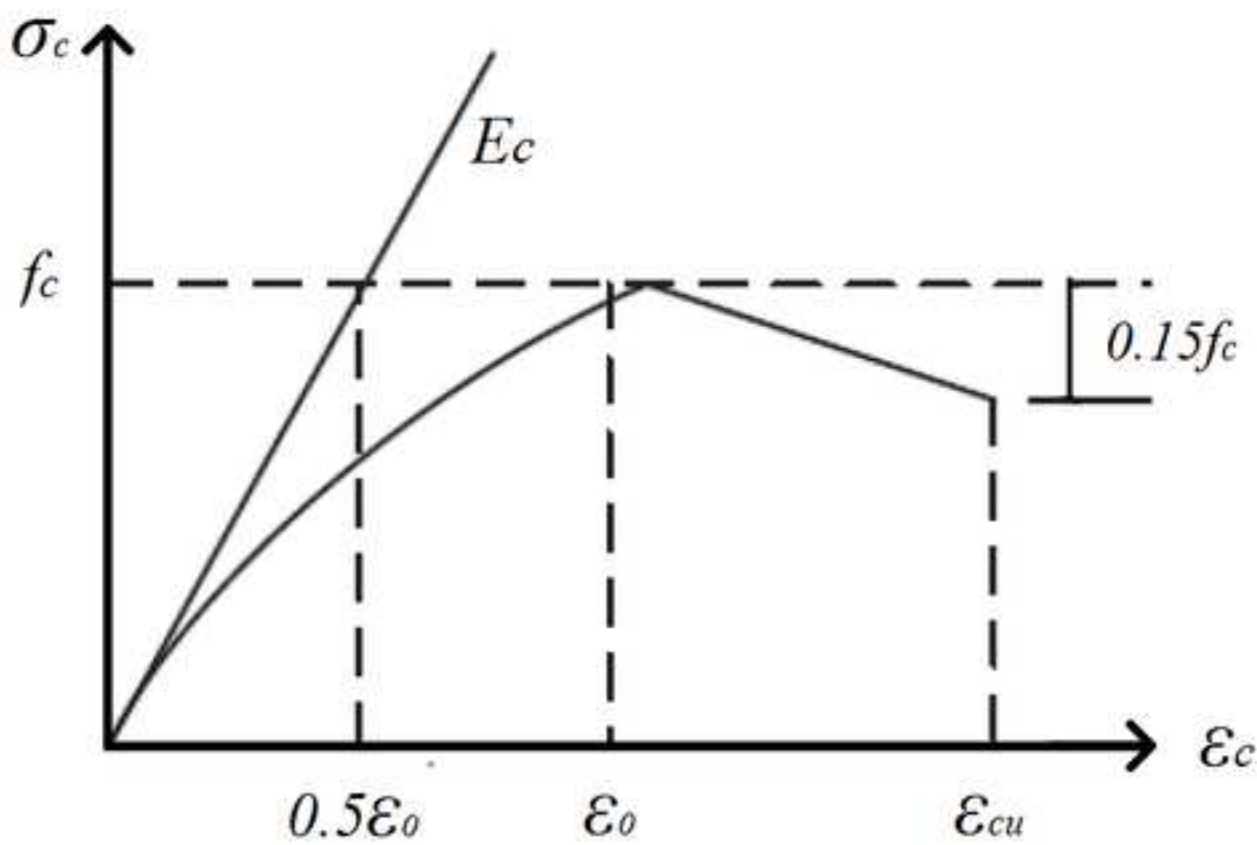


Fig. 3

[Click here to download high resolution image](#)

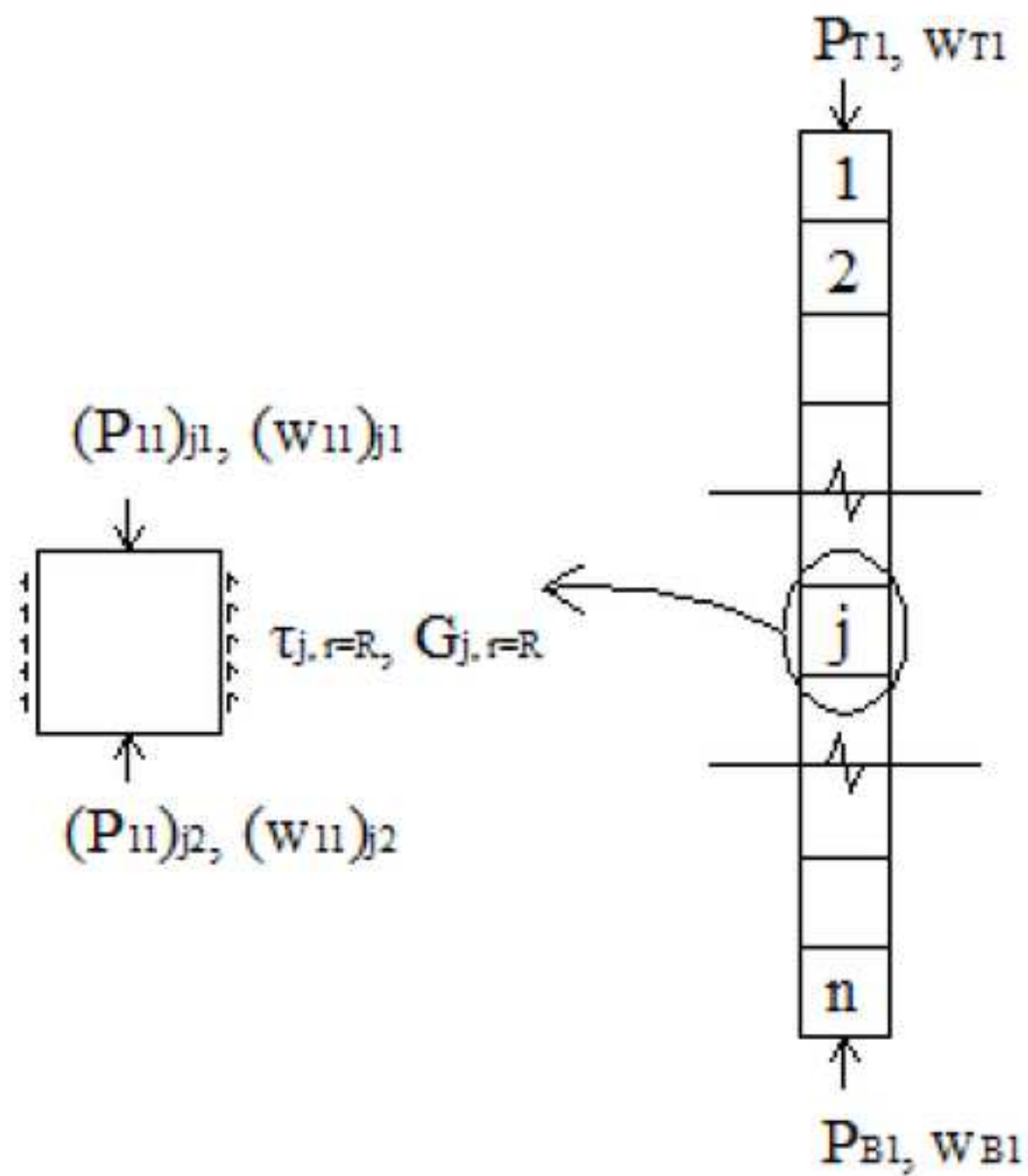


Fig. 4
[Click here to download high resolution image](#)

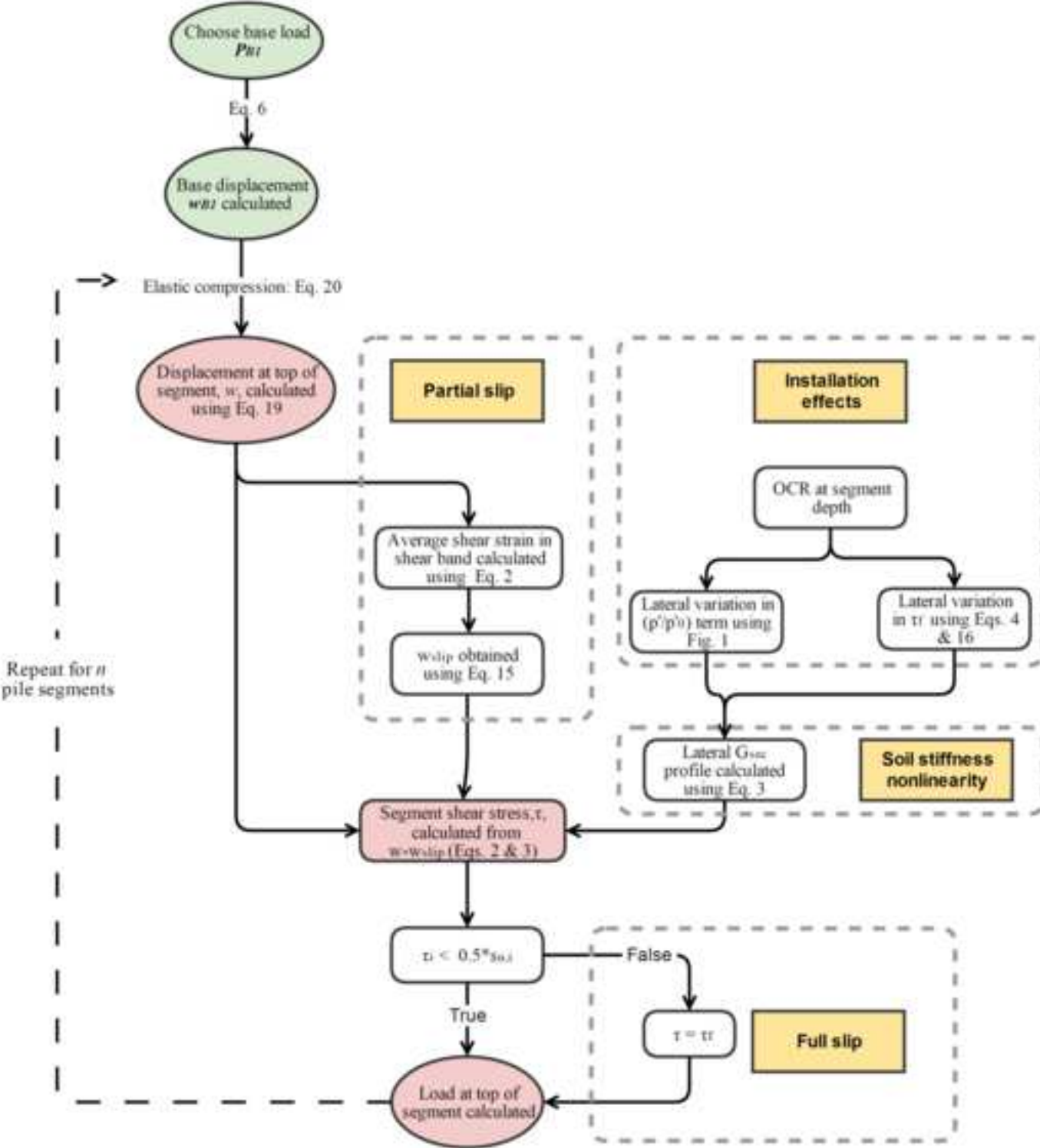


Fig. 5

[Click here to download high resolution image](#)

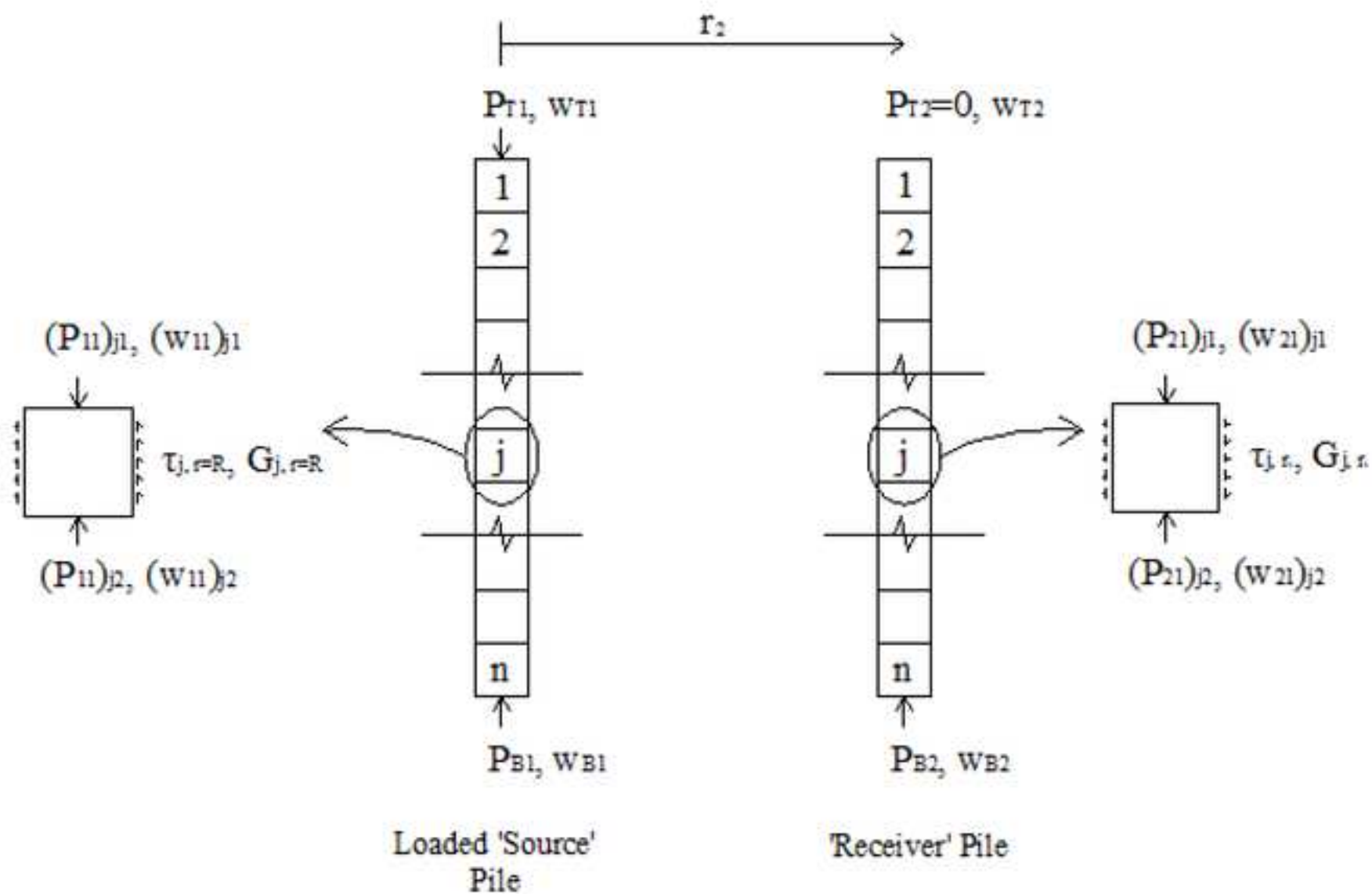


fig. 6.

[Click here to download high resolution image](#)

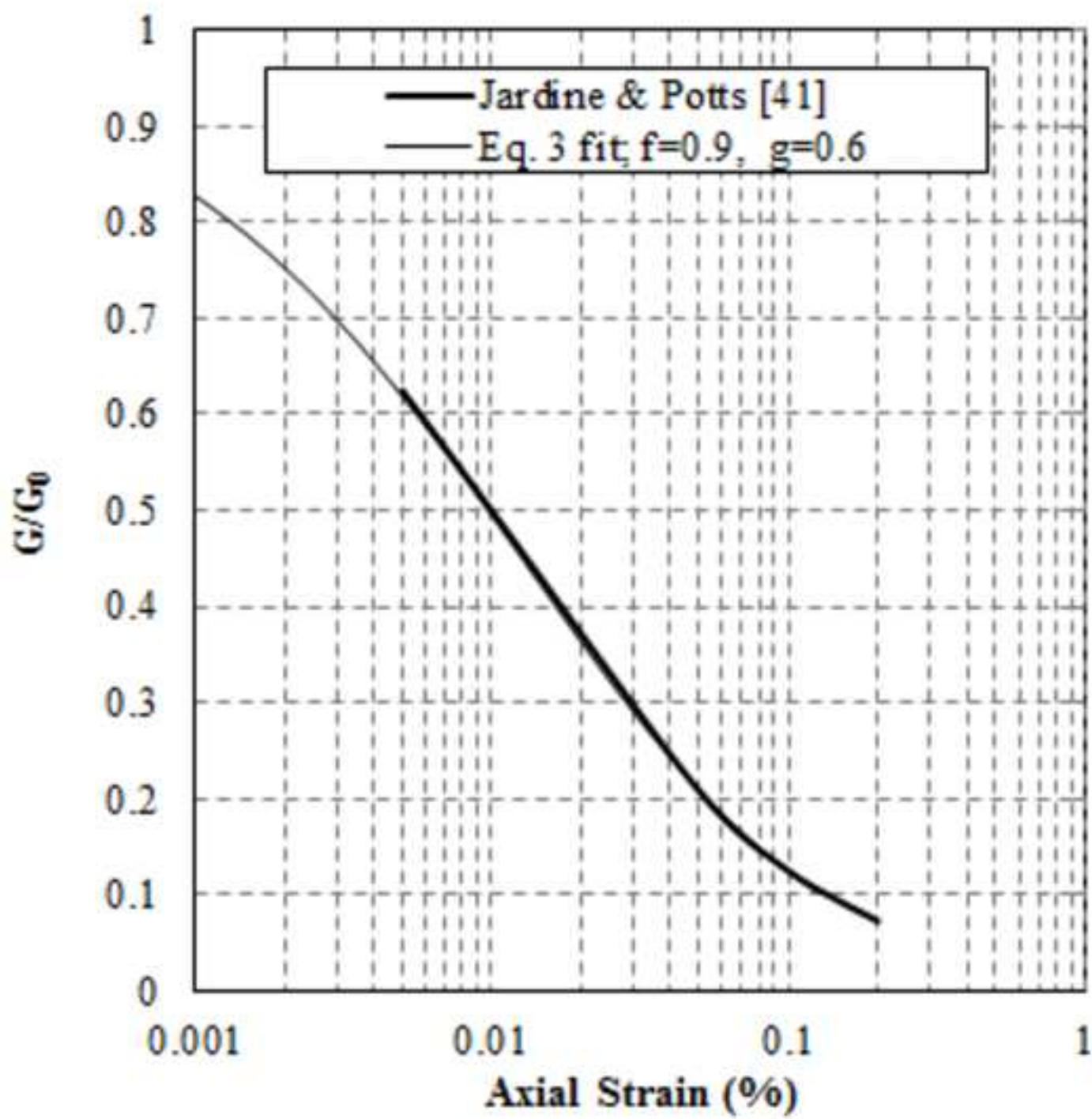


fig. 7

[Click here to download high resolution image](#)

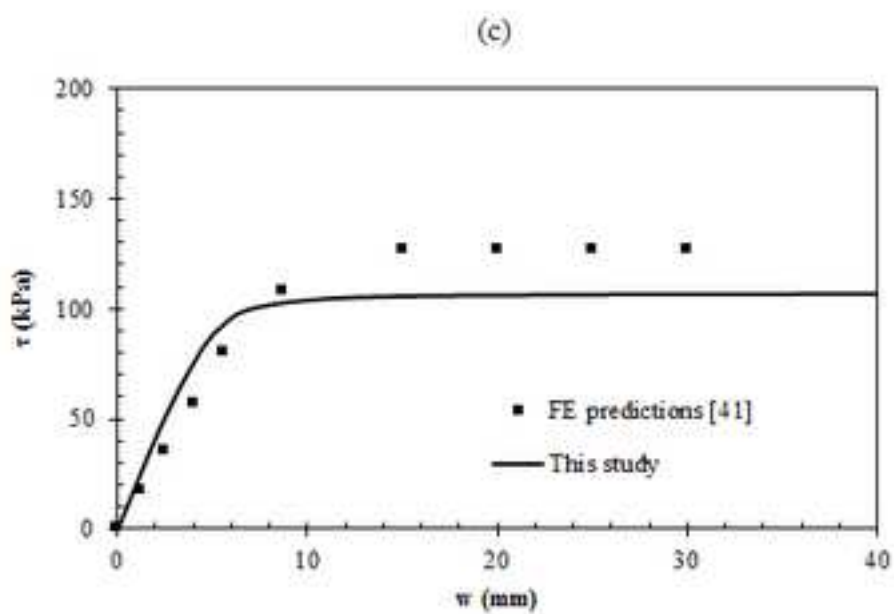
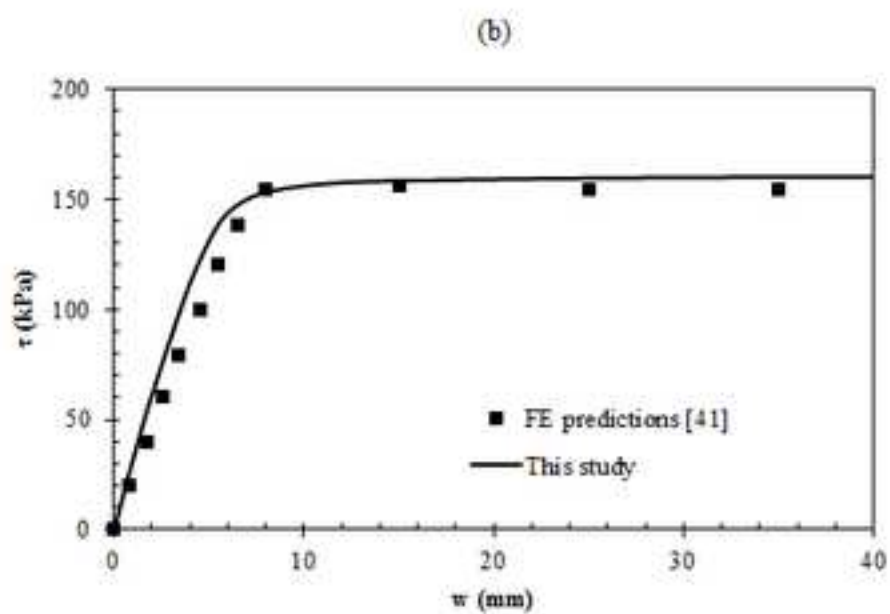
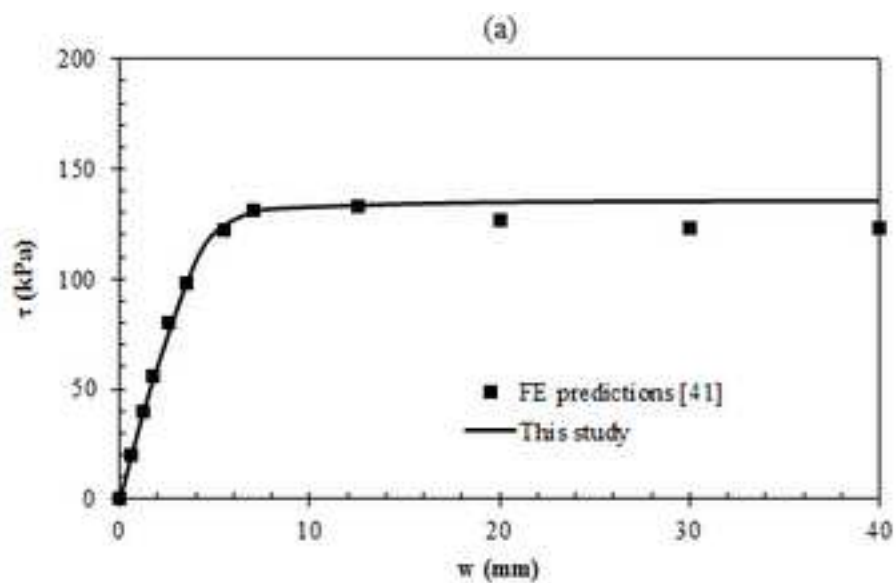


fig. 8

[Click here to download high resolution image](#)

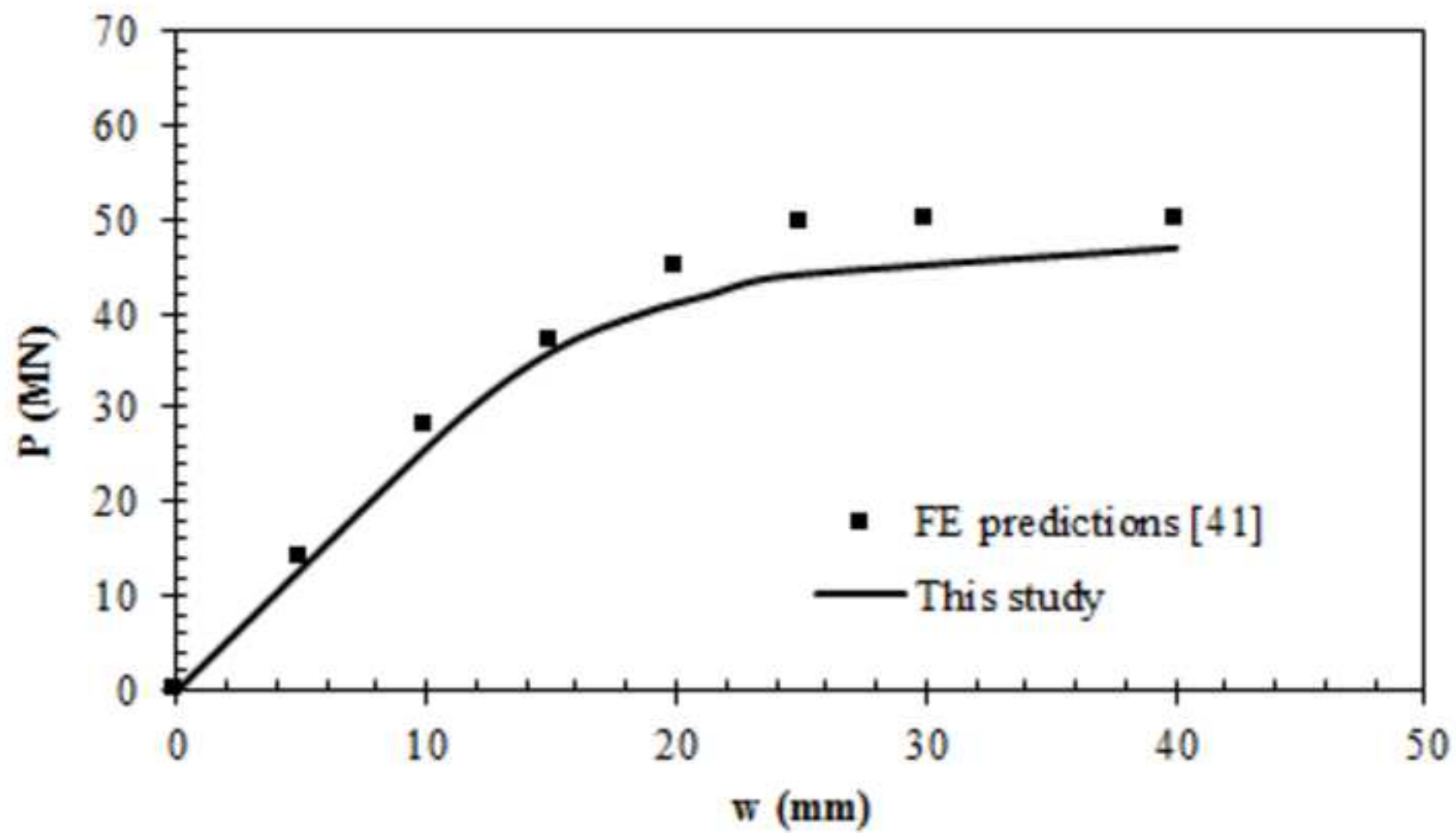


fig. 9

[Click here to download high resolution image](#)

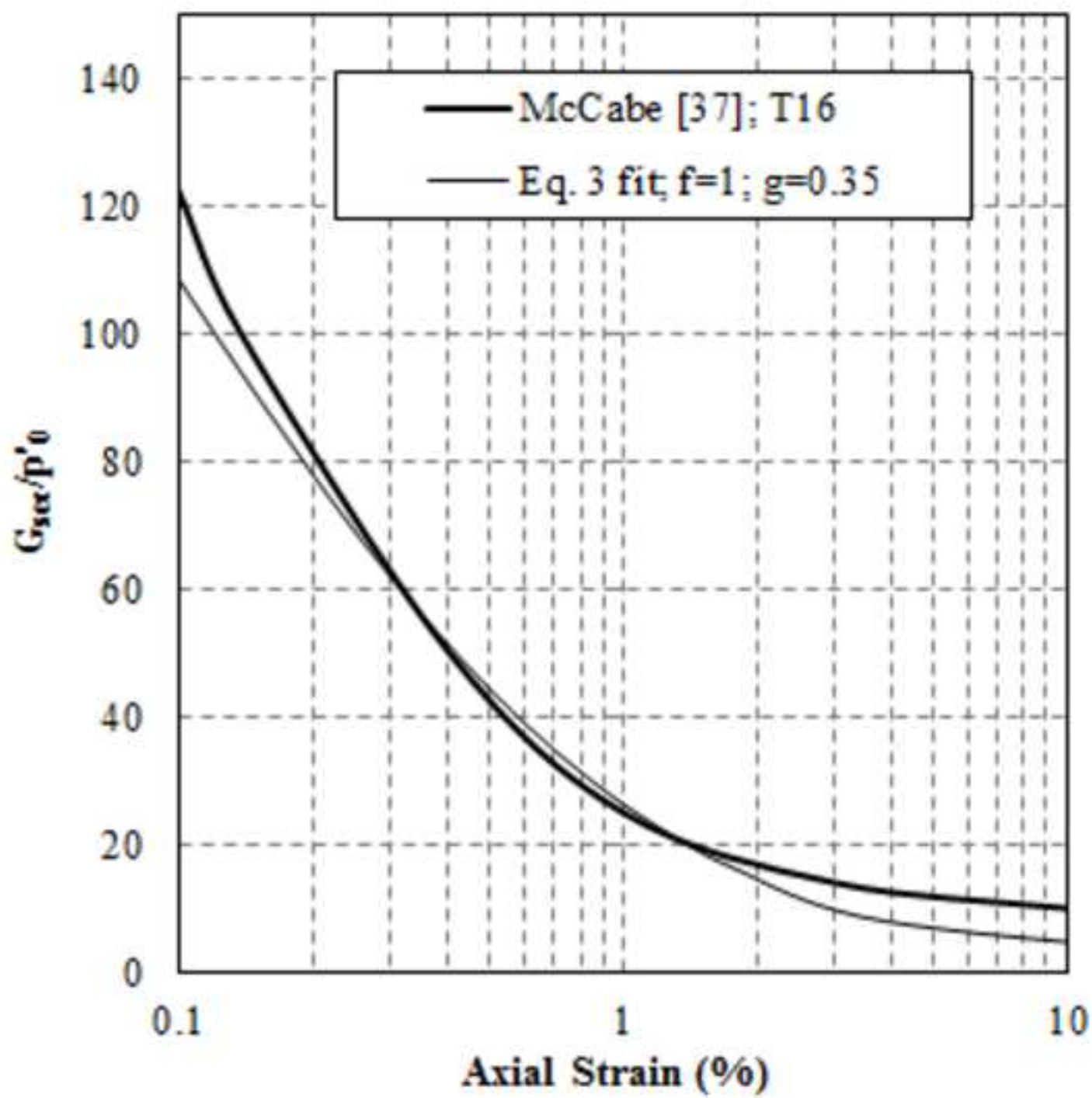


fig. 10
[Click here to download high resolution image](#)

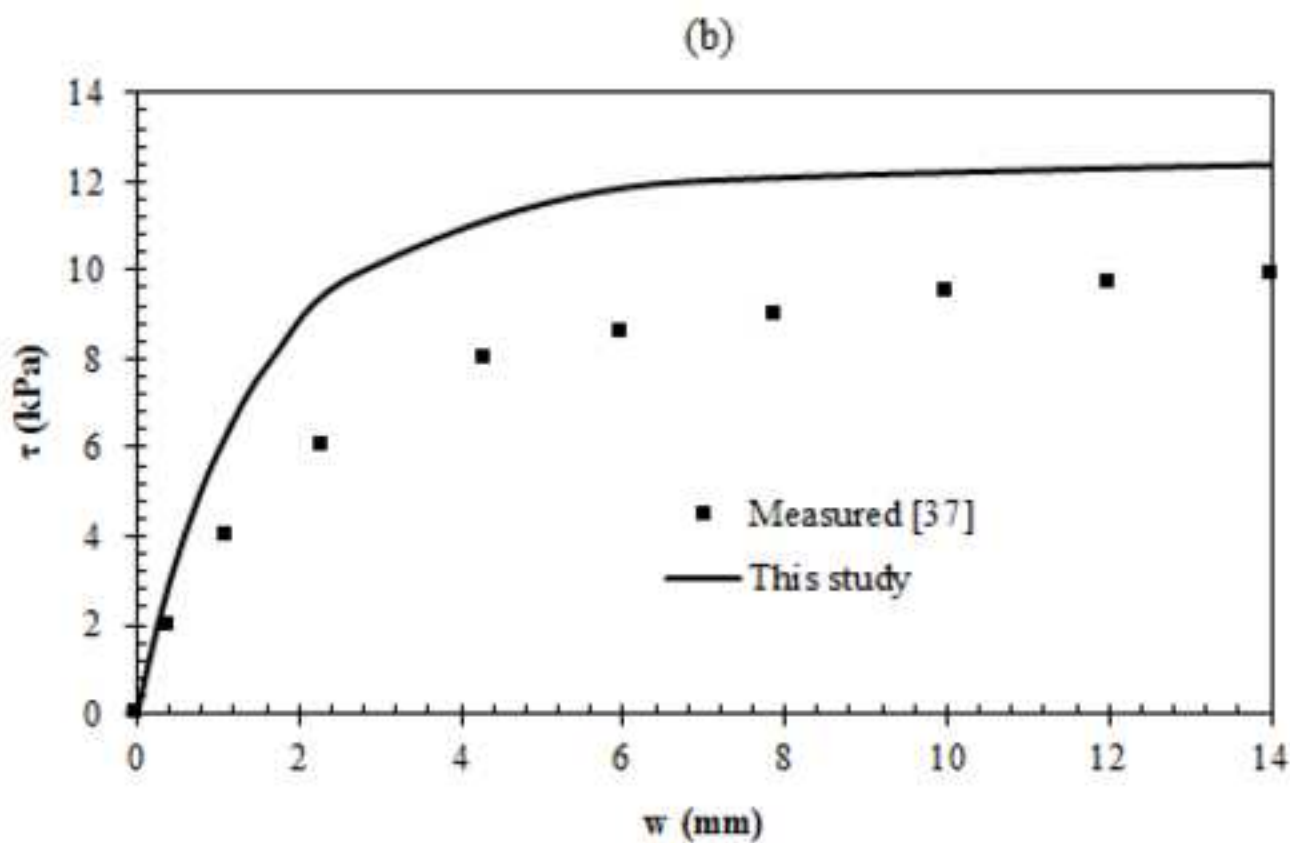
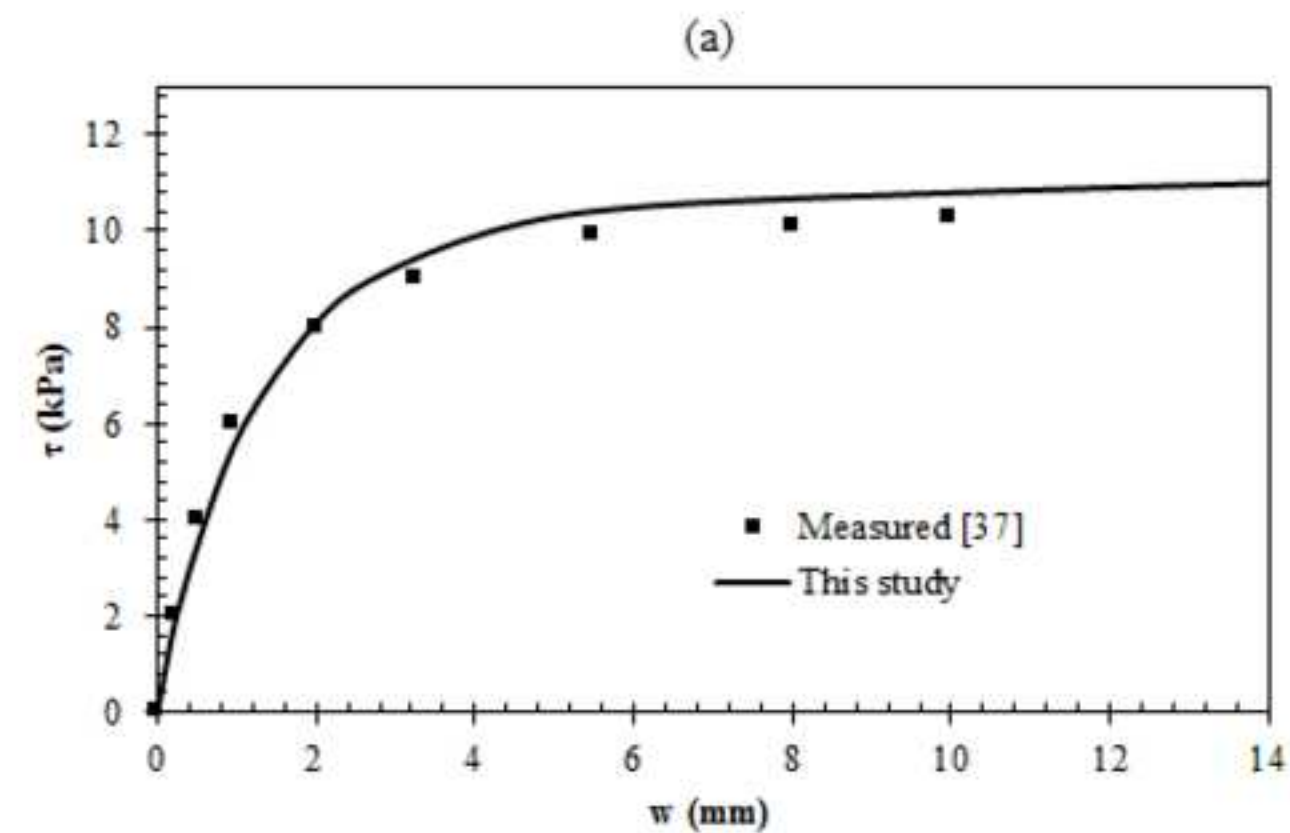


fig. 11

[Click here to download high resolution image](#)

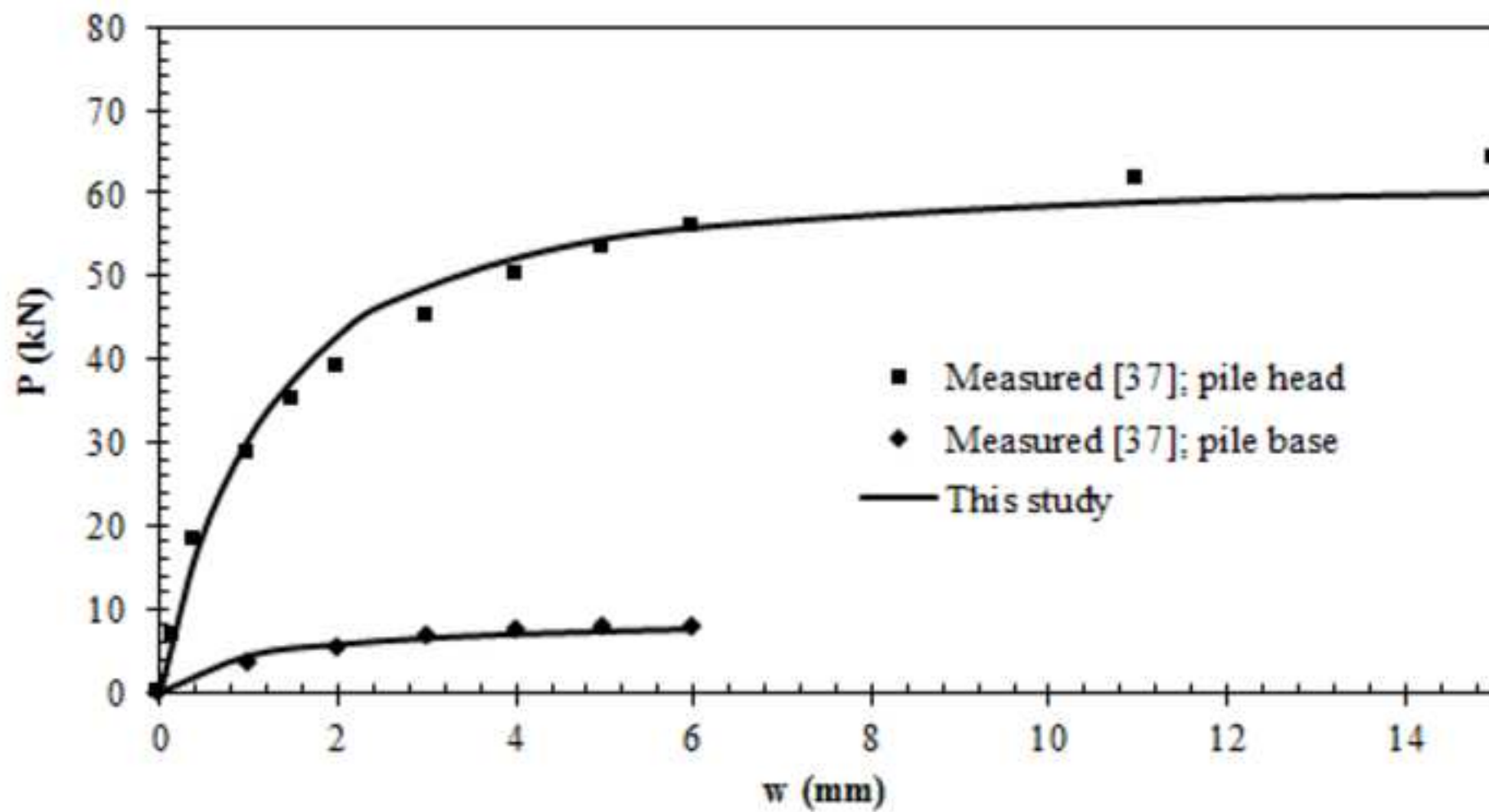


fig. 12

[Click here to download high resolution image](#)

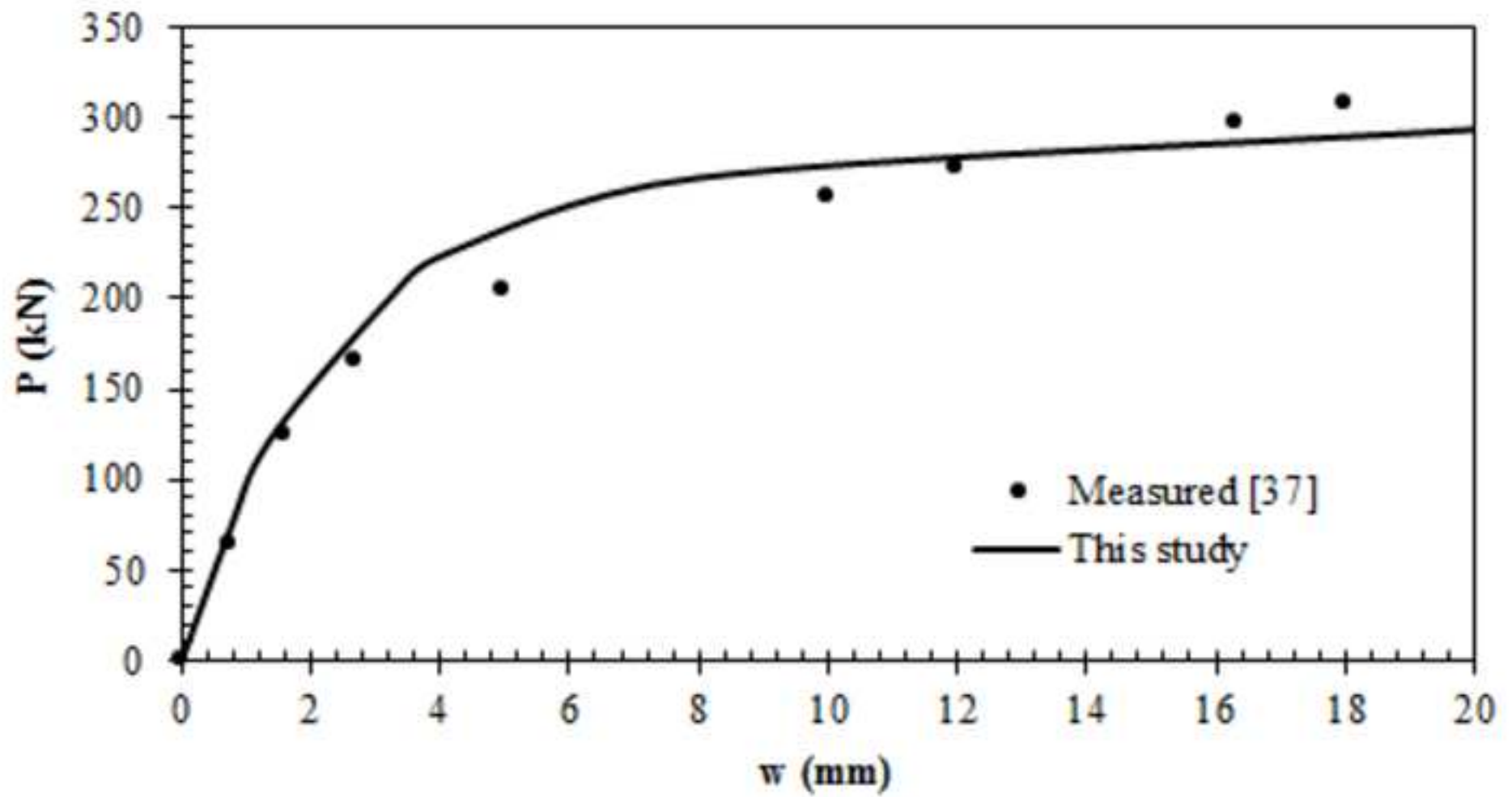


fig. 13

[Click here to download high resolution image](#)

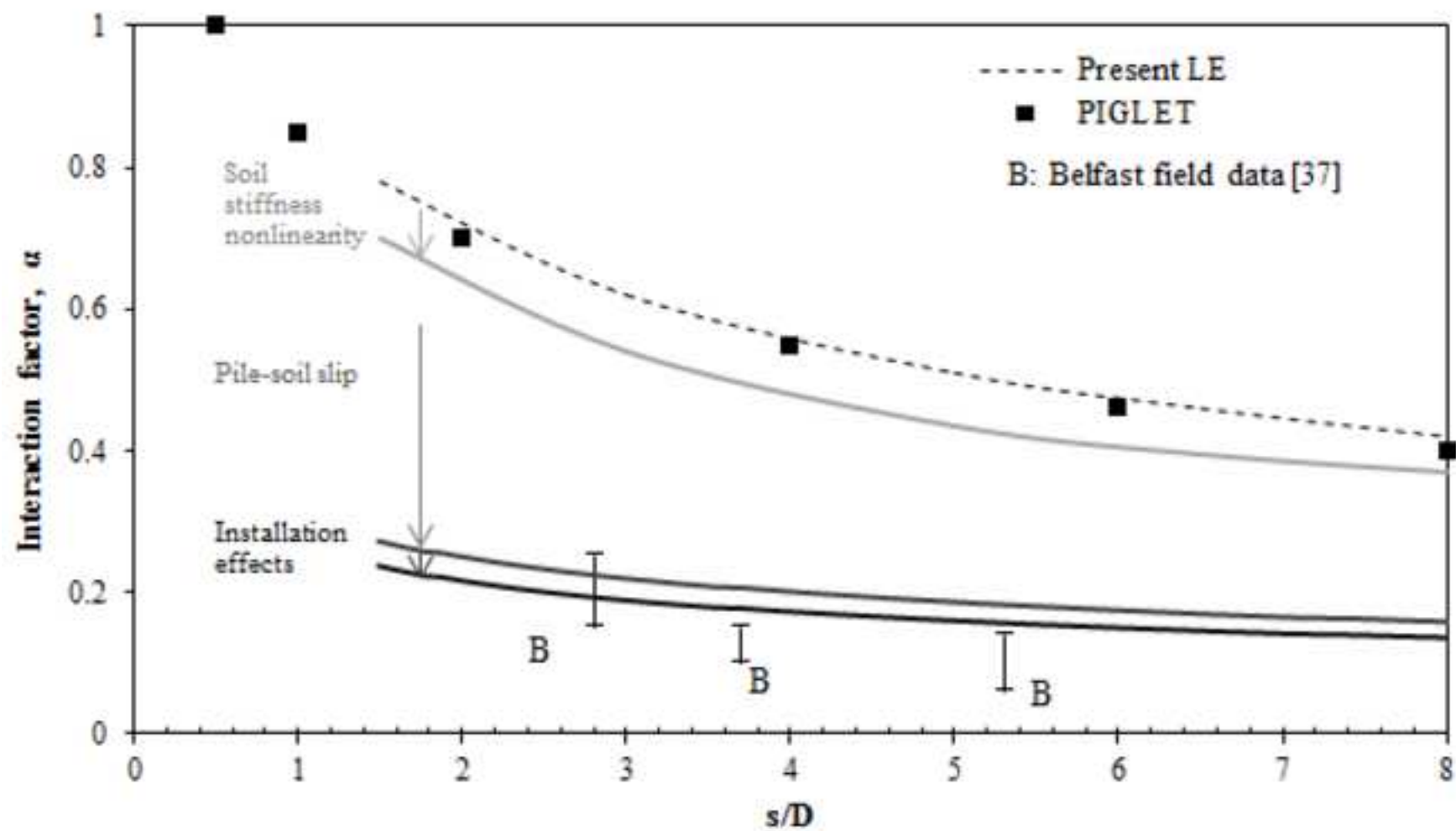


fig. 14

[Click here to download high resolution image](#)

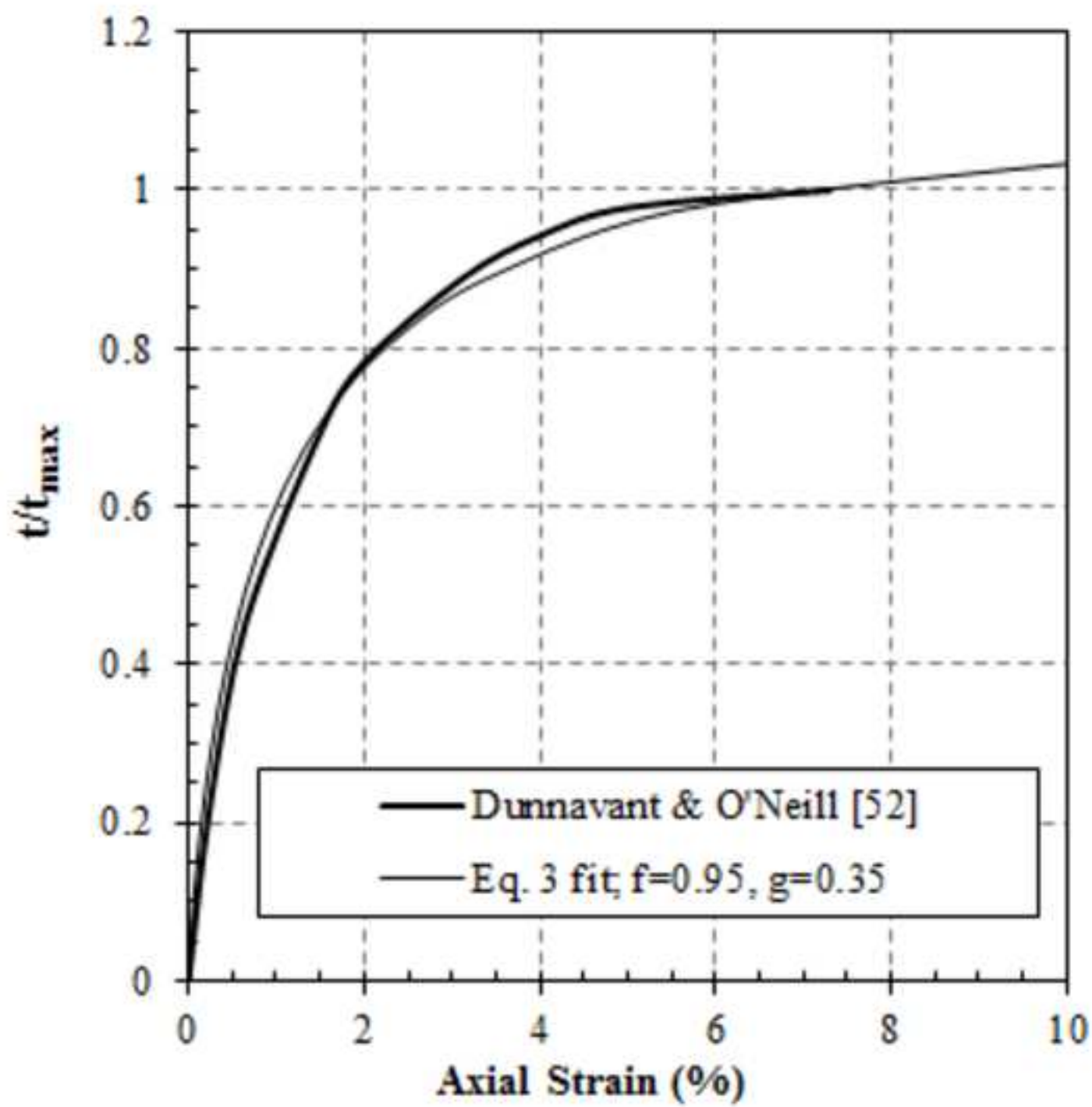


fig. 15
[Click here to download high resolution image](#)

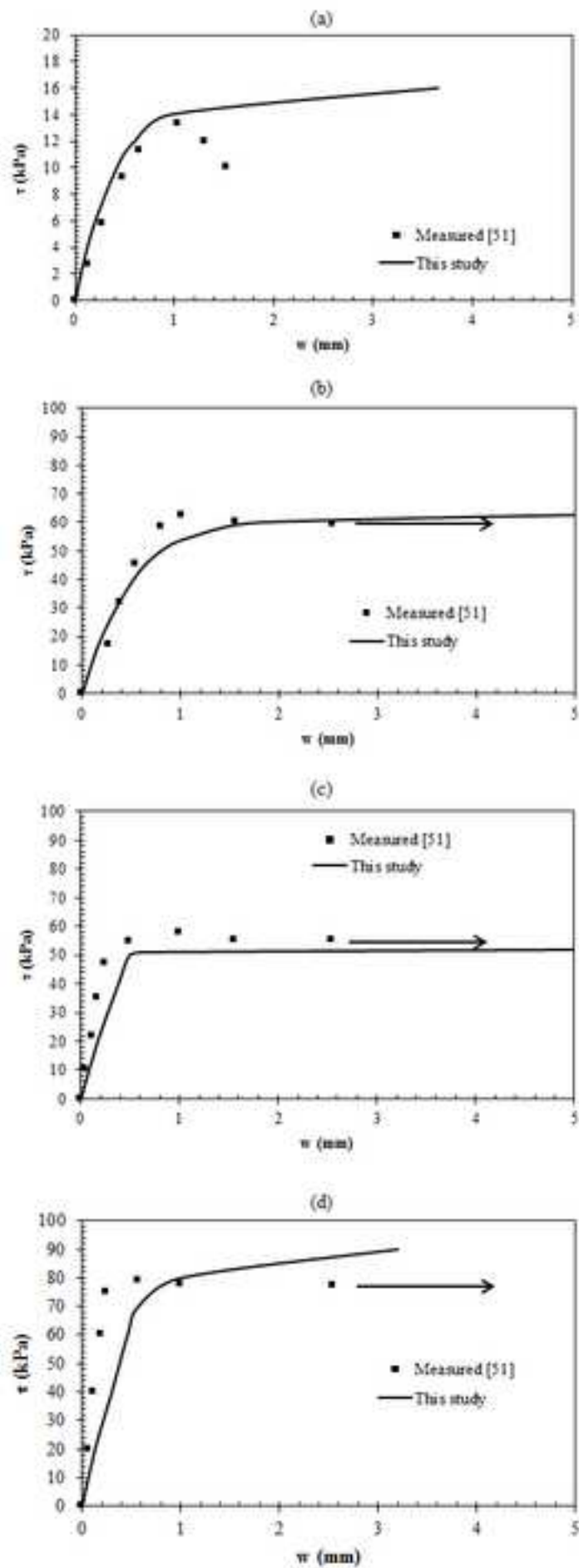


fig. 16

[Click here to download high resolution image](#)

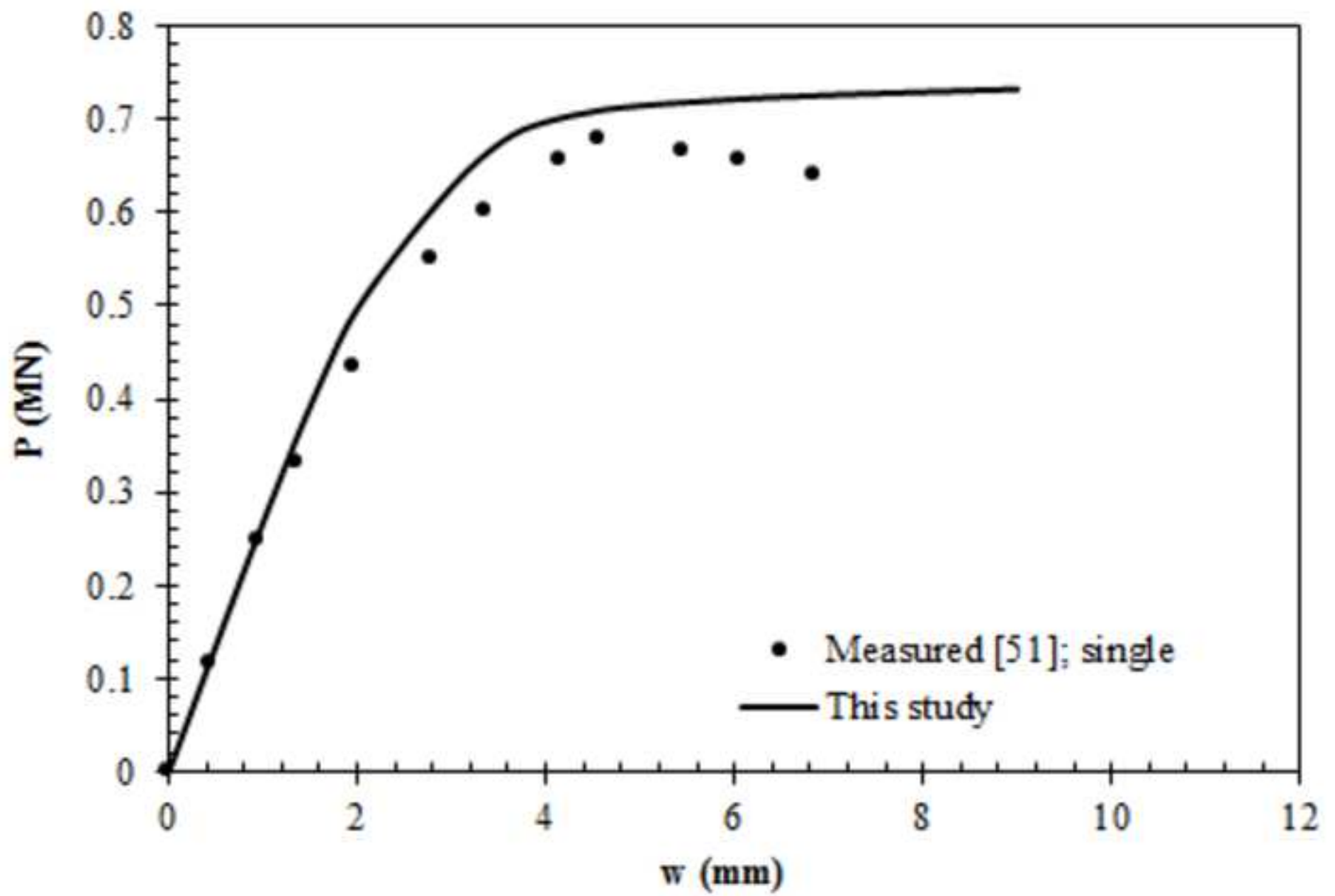


fig. 17

[Click here to download high resolution image](#)

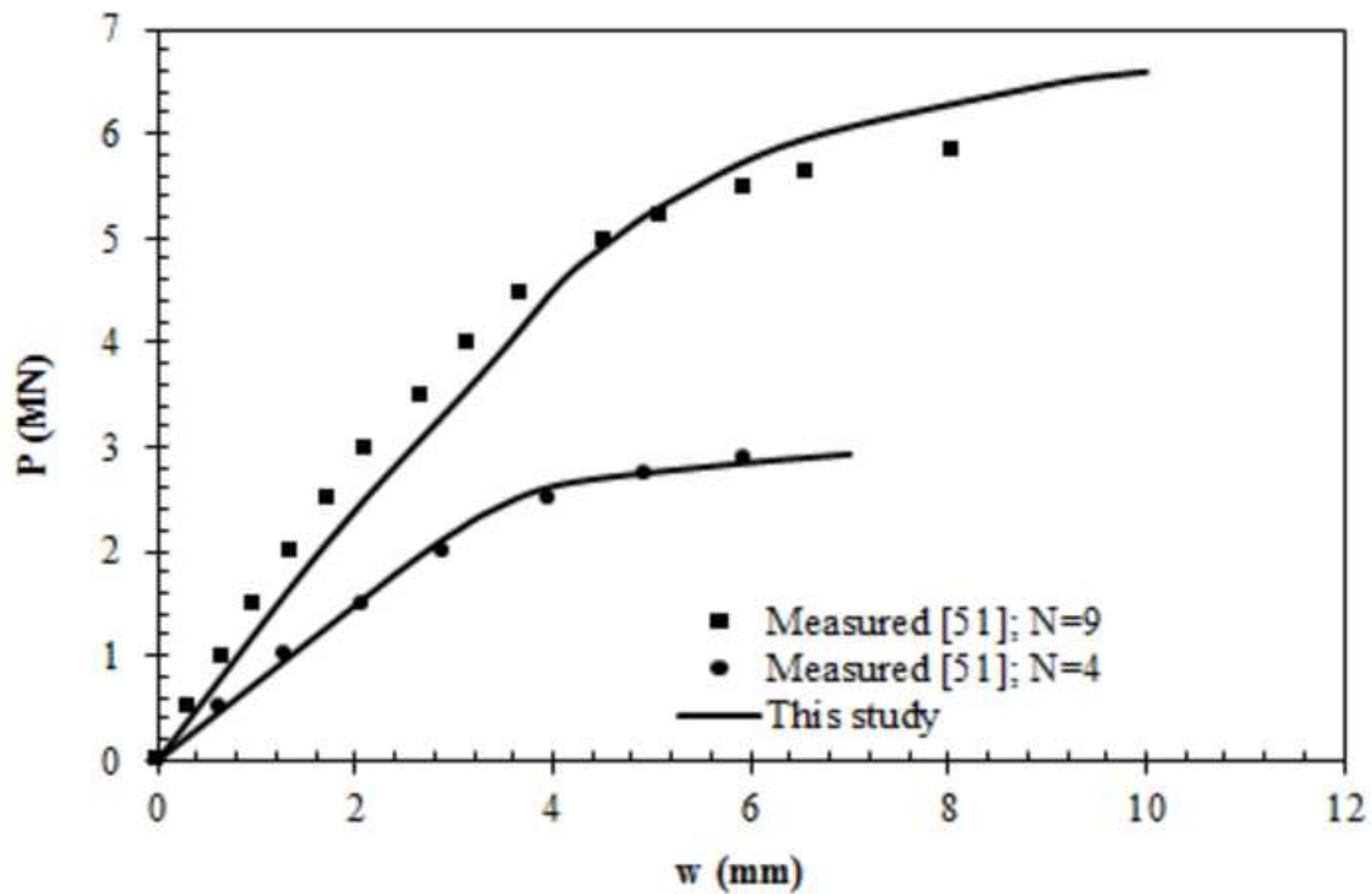


fig. 18
[Click here to download high resolution image](#)

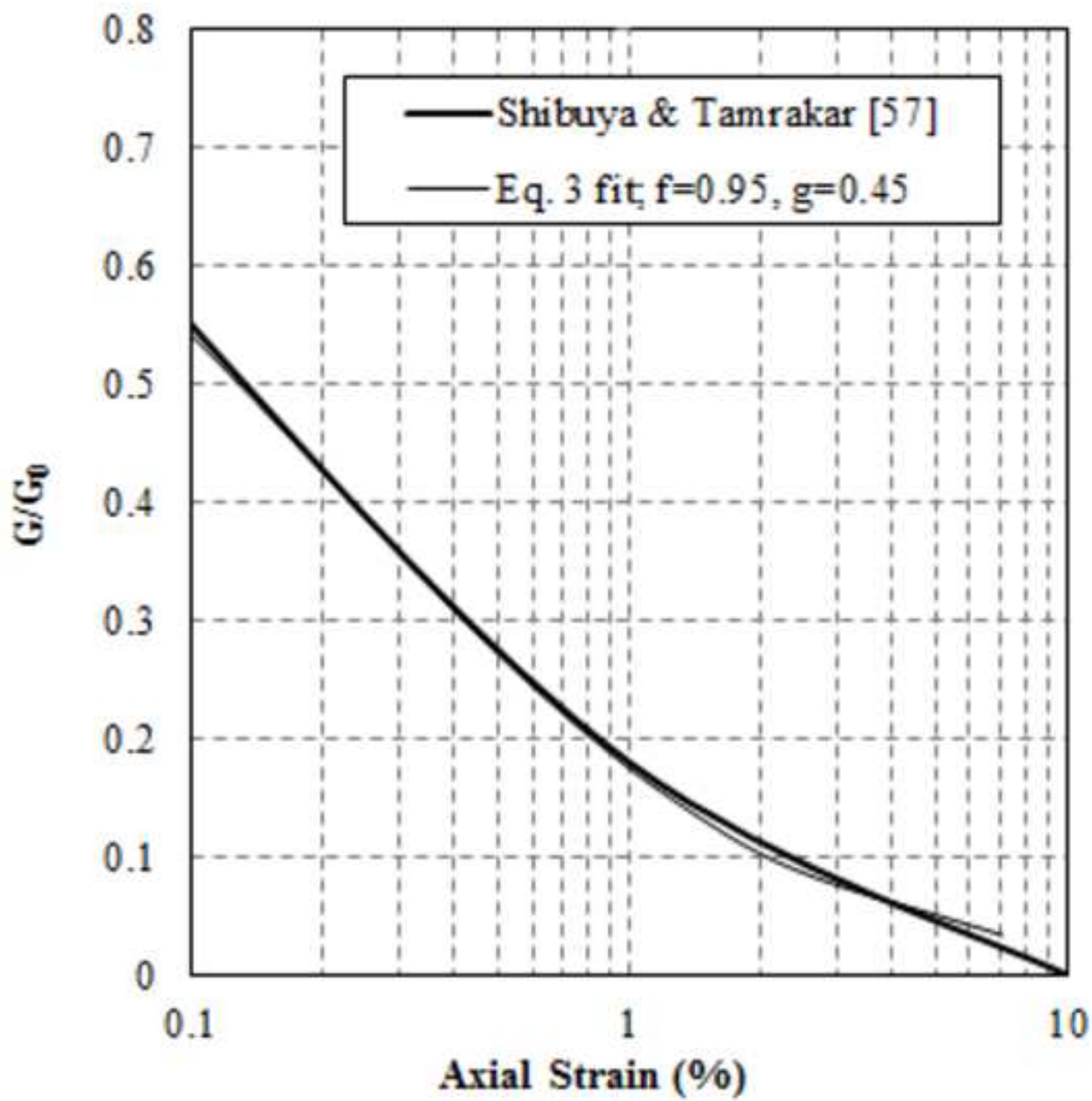


fig. 19

[Click here to download high resolution image](#)

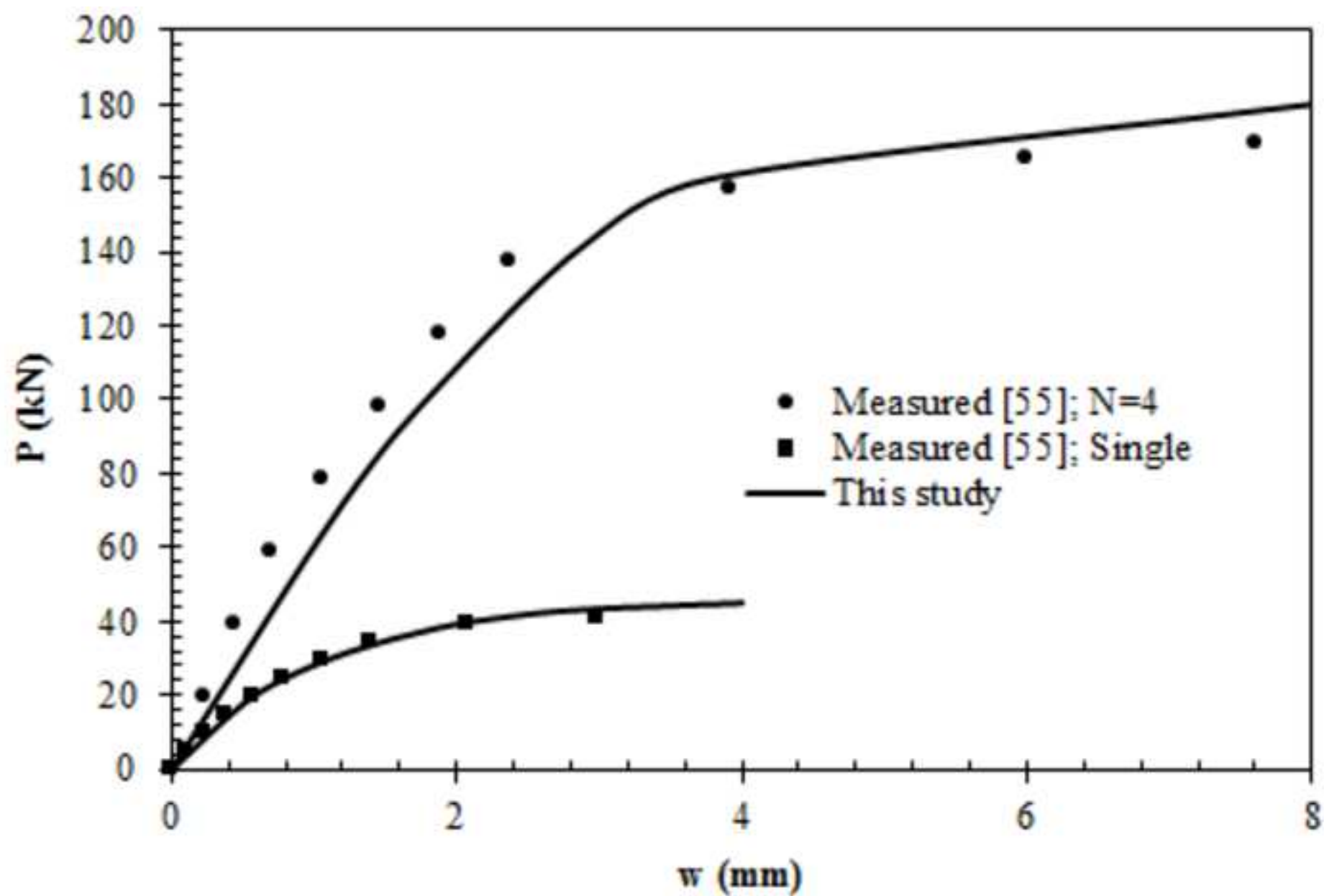


Fig. 1 FE predictions of mean effective stress distribution after consolidation (after Sheil *et al.*[23])

Fig. 2 Hognestad model (adapted from Wang et al. [14])

Fig. 3 Illustration of single pile notation

Fig. 4 Illustration of iterative process for a single loaded pile

Fig. 5 Illustration of single pile and receiver pile notation

Fig. 6 Calibration of shear modulus degradation parameters for Hutton clay

Fig. 7 Comparison between predicted single pile t-z curves determined in this study and FE analyses for (a) 16 m, (b) 28 m and (c) 47 m depths in Hutton clay

Fig. 8 Comparison between predicted single pile load-displacement behaviour determined by this study and FE analyses in Hutton clay

Fig. 9 Calibration of shear modulus degradation parameters for Belfast *sleech*

Fig. 10 Comparison between measured and predicted single pile t-z curves for (a) 3.25 m and (b) 5.25 m depths in Belfast *sleech*

Fig. 11 Comparison between measured and predicted single pile load-displacement relationships in Belfast *sleech*

Fig. 12 Comparison between measured and predicted 5-pile group load-displacement relationships

Fig. 13 Influence of various model aspects

Fig. 14 Calibration of shear modulus degradation parameters for Houston clay

Fig. 15 Comparison between measured and predicted single pile t-z curves for (a) 1 m – 2.5 m, (b) 4 m - 7 m, (c) 9 m and (d) 10 m – 12 m depths in Houston clay

Fig. 16 Comparison between measured and predicted single pile load-displacement relationships in Houston clay

Fig. 17 Comparison between measured and predicted pile group load-displacement relationships in Houston clay

Fig. 18 Calibration of shear modulus degradation parameters for Bangkok clay

Fig. 19 Comparison between measured and predicted single pile and pile group load-displacement relationships in Bangkok clay